Squeezing Codes

Ethan Lake

These notes were written mostly between May and July of 2024. Thanks to Ruihua Fan, Ehud Altman, Jong Yeon Lee, and Sunghan Ro for discussions. Extra thanks to Sunghan for teaching me about the content of Sec. 5 and for running lots of numerics (not included), and to Ruihua for helping fix an RG calculation (also not included) pertaining to the critical point of the $\mathsf{S}_{2,3}$ automata.

Contents

1 Self correcting memories from squeezing dynamics

Consider constructing a robust self-correcting classical memory in $d > 1$ spatial dimensions such that 1) the state space on each site is $\{\pm 1\}$, and 2) the dynamics are translation invariant in both space and time. The most well-known way of doing this—and indeed the only way I have seen in the literature, other than Gac's mysterious automaton—is Toom's rule. Toom's rule robustly encodes a single bit in the sign of the magnetization, and a threshold is achieved by using corner-shaped majority votes, which eliminate minority domains in a ballistic fashion by eroding them from their corners.

Toom's rule is however not the only way of robustly eroding minority domains. Toom's rule attempts to locally identify minority domains using the fact that they are convex, and hence must possess corners. In $d > 1$, it is however possible to correct minority domains *without* first identifying wether or not they belong to the minority spin species.

This is done by engineering dynamics which "squeezes" domains in an anisotropic fashion. Consider for definiteness $d = 2$. Roughly speaking, any rule which is such that

"clusters of $+1$ spins expand vertically, and clusters of -1 spins expand horizontally" (1)

will yield a self-correcting memory. Under this dynamics, a minority $+1$ domain will be made progressively narrower along the x direction until it is eventually destroyed, while a minority -1 will be similarly destroyed by shrinking along the y direction (see Fig.1). Generalizations to $d > 2$ dimensions are straightforward: as long as there are distinct directions along which both $+1$ and -1 spins expand, self-correcting dynamics can be achieved.

1.1 Automaton dynamics: synchronous and asynchronous updates

The models considered in these notes will all be formulated within the context of discrete-time probabilistic cellular automaton dynamics, which we now define. Each model will be defined by an automaton rule A that determines how spins are updated in the absence of noise. The rule A gives a set of instructions for determining how the spins are to be updated, viz. it specifies a set of functions $f_i(\{s_j(t)\})$ that determine $s_i(t+1)$ in terms of the spins at time t (these functions may be stochastic, with e.g. a random type of update being chosen at each step). All of the models we consider will have translation-invariant update functions for which $s_i(t+1)$ is determined only by those $s_j(t)$ with j an $O(1)$ number of sites away from i.

There are two main classes of automata dynamics that we will consider, distinguished by whether the updates occur in a coordinated or uncoordinated fashion across all lattice sites.

Definition 1. A *synchronous* automaton $\mathsf{A}_{\text{synch}}$ performs a simultanous update of all spins at each time step:

$$\mathsf{A}_{\text{synch}} \; : \; s_i(t+1) = f_i(\{s_j(t)\}) \qquad \forall\, i. \tag{2}$$

Definition 2. An *asynchronous* automaton $\mathsf{A}_{\text{asynch}}$ operates by randomly choosing lattice sites at which to update spins. In a system of N spins, it most naturally proceeds in time steps of length $1/N$, where at each step,

$$\mathsf{A}_{\text{asynch}} \; : \; s_i(t+1/N) = \begin{cases} f_i(\{s_j(t)\}) & \text{with prob.} \quad 1/N \\ s_i(t) & \text{with prob.} \quad 1-1/N \end{cases} \tag{3}$$

We will model the effects of noise by assuming that each time a spin is updated, it is updated to the (correct) value determined by the update rule in question with probability $1-p$, and with probability p is replaced by a Bernoulli random variable with bias η. Thus whenever the clean dynamics instructs us to replace $s_i(t)$ by $f_i(\{s_j(t)\})$, we instead do

$$s_i(t) \mapsto \begin{cases} f_i(\{s_j(t)\}) & \text{with prob.} \quad 1-p \\ \pm 1 & \text{with prob.} \quad p\dfrac{1 \pm \eta}{2} \end{cases} \tag{4}$$

Our threshold theorems will not depend on assuming this form spacetime iid noise—indeed they will only require stochastic p-bounded noise for some $O(1)$ value of p[1]—but for simplicity we will specify to this type of noise throughout.

1.2 Two squeezing rules

We now concretely define two types of squeezing codes $\mathsf{S}_2, \mathsf{S}_3$ that we will study extensively in the following. Both rules are most naturally formulated in a Floquet fashion: for synchronous updates, the dynamics applies +1 spin expanding updates on

[1] Meaning that at each time step, the probability for a collection of M spins to be updated in a way which disagrees with the noise-free automaton rule is upper bounded by p^M.

even time steps, and -1 spin expanding updates on odd time steps (for asynchronous updates, the type of update is chosen randomly).

To write down the update rules, it will be convenient to use logical notation where a $+1$ spin is regarded as true and a -1 spin is regarded as false. In two dimensions, the S_2 rule (with synchronous updates) is defined as

$$\mathsf{S}_2 \,:\, s_{x,y}(t+1) = \begin{cases} s_{x+1,y}(t) \,\wedge\, s_{x-1,y}(t) & t \in 2\mathbb{Z} \\ s_{x,y+1}(t) \,\vee\, s_{x,y-1}(t) & t \in 2\mathbb{Z}+1 \end{cases} \tag{5}$$

The other automaton we will focus on is defined by adding on the site to be updated to the RHS:

$$\mathsf{S}_3 \,:\, s_{x,y}(t+1) = \begin{cases} s_{x+1,y}(t) \,\wedge\, s_{x,y}(t) \,\wedge\, s_{x-1,y}(t) & t \in 2\mathbb{Z} \\ s_{x,y+1}(t) \,\vee\, s_{x,y}(t) \vee\, s_{x,y-1}(t) & t \in 2\mathbb{Z}+1 \end{cases} \tag{6}$$

As mentioned above, for asynchronous updates, a random type of update (vertical or horizontal) is chosen at each site. We will always take the probabilities of vertical and horizontal updates to be equal; favoring one type of update over the other has essentially the same effects as modifying the strength and bias of the noise.

The differences between $\mathsf{S}_2, \mathsf{S}_3$ are superficially rather minor, but interestingly will be seen to lead to very different physics.

Both of these rules—and more generally, any squeezing rule—break detailed balance. To show this, it is sufficient to find a closed loop of states A_i, $i = 1, \ldots, n$ in configuration space $A_1 \to \cdots \to A_1$ such that $\prod_{i=1}^{n} P(A_i \to A_{i+1})/P(A_{n-i+1} \to A_{n-i}) \neq 1$. One such loop is displayed below for the S_2 rule at $\eta = 0$; the arrows indicate the respective transition probabilities (multiplied by the system size) for asynchronous updates:

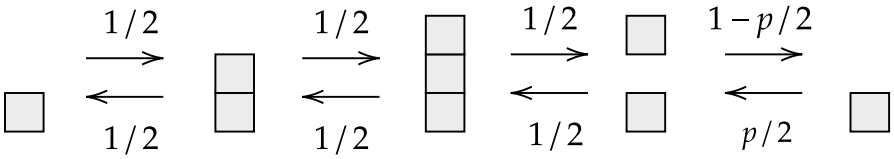

(7)

where the gray squares represent $+1$ spins in a background of -1 spins. For this sequence $\prod_{i=1}^{n} P(A_i \to A_{i+1})/P(A_{n-i+1} \to A_{n-i}) = 2/p - 1$, which breaks detailed balance except in the trivial ("infinite temperature") case where $p = 1$. When $p = 0$ so that the dynamics is error-free, the loop around which the system travels following the $\to$ arrows is irreversible, automatically implying that DB is broken.

These automata are dinstinct from Toom's rule in a few ways. One is in terms of symmetries: instead of the internal $\mathbb{Z}_2$ spin-flip symmetry of Toom's rule, these rules possess only a mixture of a $\mathbb{Z}_2$ spin flip and C_4 rotation symmetry, generated by

$$\widetilde{R}_{\pi/2} = R_{\pi/2} \circ X \tag{8}$$

where X performs a global spin flip (there are other squeezing automata which lack this symmetry but nevertheless possess thresholds). Another difference is that these

rules do not involve majority voting. A third difference is that unlike Toom's rule, minority domains with an aspect ratio of < 1 or > 1 (depending on their spin) will get bigger before they are eliminated, so the magnetization may not be monotonic in time even in the absence of errors. As an extreme example, a minority domain of -1 spins that spans the system vertically will always grow to overwhelm the system, no matter how thin the initial domain is[2] (and the analogous $\pi/2$-rotated statement for a minority $+1$ domain). This example shows us a further distinction: in Toom's rule a homologically-nontrivial straight strip of minority spins never gets erased under noise-free dynamics, meaning that the noise-free system possesses (extensively many) distinct fixed points under periodic boundary conditions. The noise-free $\mathsf{S}_2, \mathsf{S}_3$ by contrast possesses only two absorbing states.[3]

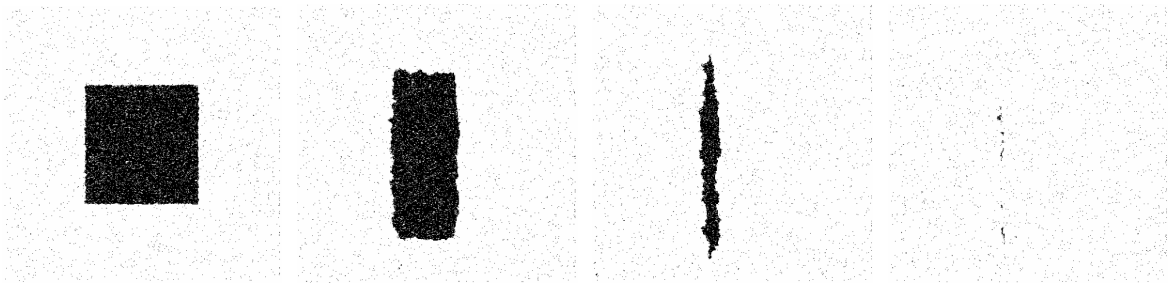

Figure 1: Elimination of a minority domain under asynchronous S_3 in a system of size $L = 500$ with unbiased noise of strength $p = 0.2$. Performing a global spin flip on the initial configuration would result in the domain being squeezed in the orthogonal direction.

1.3 Threshold theorems for synchronous updates

In this section we prove that any *synchronous* automaton that squeezes domains in the way defined above constitutes a robust self-correcting memory.

To discuss the proof, we need some notation. A necessary (but not sufficient) condition for an automaton A to possess a threshold is that it be able to correct against minority domains of errors in the *absence* of noise. This is formalized in the following definition:

Definition 3. Let $|\overline{\pm 1}\rangle$ be the state of an infinite system in which all spins are ± 1. Consider any spin configuration obtained by starting with $|\overline{-1}\rangle$ and flipping a finite number of spins to $+1$. An automaton A is an *eroder* if 1) in the absence of errors, the action of A on any such state produces $|\overline{-1}\rangle$ in finite time, and 2) A leaves $|\overline{-1}\rangle$ invariant.

[2] This is true for the S_3 rule; for S_2 the domain needs to be at least two sites thick.

[3] Toom can be "fixed" in this regard by simply putting it on a different lattice; this is the content of Kubica and Preskill's paper [4] (which does not provide a local decoder for the 3d TC, despite the abstract). A different fix is to just add in below-threshold noise; this coarsens and then destroys the strips.

Squeezing codes are all eroders: this follows simply because the region of $+1$ spins is bounded by a rectange whose width (but not necessarily height) decreases linearly with time (in the absence of errors).

For memories, we are interested in computing the relaxation times $\tau(\sigma)$ of the two logical states:

$$\tau(\sigma) = \min\{t \,:\, \mathbb{E}(\sigma M(t)) < \varepsilon),\ M(0) = \sigma\}, \tag{9}$$

where $M(t) = \sum_i s_i/L^2$ is the magnetization, $\mathbb{E}$ is over noise realizations, ε is an arbitrary $O(1)$ constant, and $\sigma = \pm 1$ determines the logical state in which the memory is initialized.

We can prove bounds on $\tau(\sigma)$ using old results from Toom. First, note that the rules $\mathsf{S}_2, \mathsf{S}_3$ are *monotone*, meaning that they are determined by monotone Boolean functions.[4] When then use the following (very nontrivial) theorem of Toom (see also [5] for a more accessible exposition):

Theorem 1 (Toom, [8])**.** *All monotone two-state eroders are robust, meaning that there exists a p_c such that when $p < p_c$, a system intitialized in $|\overline{-1}\rangle$ has the magnetization remains bounded away from 0 from below by an $O(1)$ constant for long times. More precisely, for a system of linear size L,*

$$\mathsf{A} \text{ a monotone two-state eroder} \implies \tau(-1) = \omega(L^0). \tag{10}$$

In practice we expect τ to be not just divergent but in fact to scale superpolynomially in system size. Indeed, for all memories explicitly considered in this work, we will always have $\tau \sim \exp(L^\alpha)$ for some $O(1)$ constant α.

The above definition about eroders singles out only the logical state $|\overline{-1}\rangle$. To discuss how the $|\overline{+1}\rangle$ logical state is treated, to each automaton A, we define the *dual* automaton $\mathsf{A}^\vee$ as the automaton whose transition rules obtained by negating those of A; schematically $\mathsf{A}^\vee = \neg\mathsf{A}\neg$. Thus for example

$$\mathsf{S}_2^\vee \,:\, s_{x,y}(t+1) = \begin{cases} \neg(\neg s_{x+1,y}(t) \,\wedge\, \neg s_{x-1,y}(t)) = s_{x+1,y}(t) \vee s_{x-1,y}(t) & t \in 2\mathbb{Z} \\ \neg(\neg s_{x,y+1}(t) \,\vee\, \neg s_{x,y-1}(t)) = s_{x,y+1}(t) \wedge s_{x,y-1}(t) & t \in 2\mathbb{Z}+1 \end{cases} \tag{11}$$

which is just the $\pi/2$-rotated version of S_2. This definition is needed because being a robust eroder is not enough to serve as a memory: it only guarantees that one of the two logical states (viz. $|\overline{-1}\rangle$) is preserved under noise (a well-known example of a robust eroder which does *not* function as a memory is Stavskaya's model).

For an automaton A to have a robust memory, we need both A and $\mathsf{A}^\vee$ to be eroders. This is clearly true for $\mathsf{S}_{2,3}$, since $\mathsf{S}_{2,3}^\vee$ are obtained from $\mathsf{S}_{2,3}$ by a $\pi/2$ rotation. Therefore

Theorem 2. *The automata $\mathsf{S}_{2,3}$ possess a nonzero threshold under synchronous updates.*

[4] Viz. those such that changing inputs from -1 (false) to $+1$ (true) cannot decrease the value of the output. Any function made only from $\wedge$s and $\vee$s (without any $\neg$s) is montonone because both $\wedge$ and $\vee$ are monotone.

More generally, this will be true for any automaton which performs both +1 and −1 squeezing rules along at least two independent directions (the number of +1 and −1 squeezing directions needn't be the same). Thus any such "squeezing code" will possess a nonzero threshold (again, at least for *synchronous* updates).

We now verify this numerically for S_3, by studying the behavior of the relaxation time τ of the least-stable logical state: $\tau \equiv \min_\sigma \tau(\sigma)$ (a much more detailed numerical analysis of both models appears in Sec. 4). Below threshold, we fit this as a function of linear system size L to a function of the form

$$\tau \sim e^{\alpha_L / p}. \tag{12}$$

For the S_3 update rule with unbiased noise ($\eta = 0$) and synchronous updates, we find

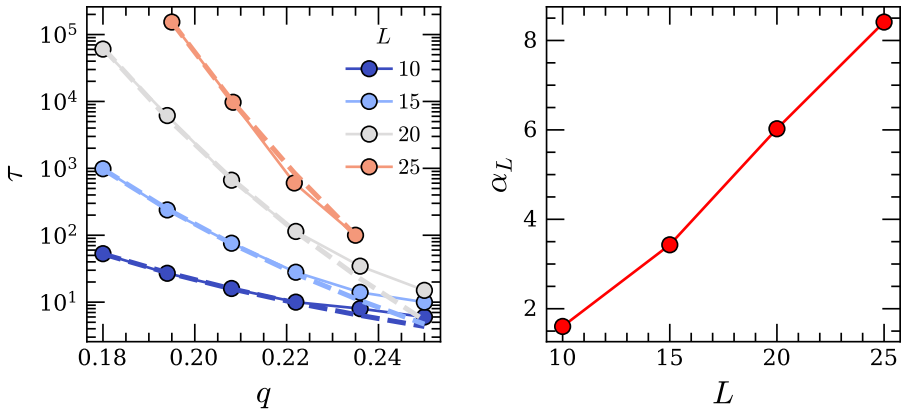

(13)

where the dashed lines are fits to the expected exponential form. Note that we indeed have $\alpha_L \propto L$, so that the divergence of τ is quite rapid below threshold.

With a (quite strong) bias of $\eta = 1/2$, we find (note: x axis label should be p)

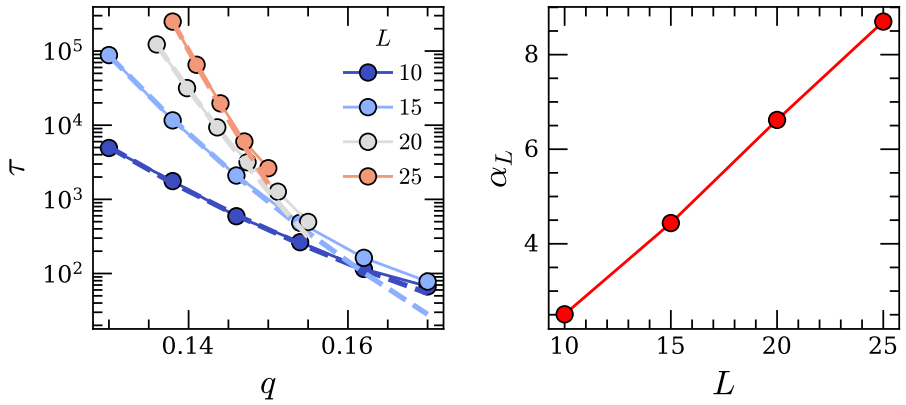

(14)

so that the same scaling with q and L is obtained, just with the threshold moved lower (albeit to still a rather high value of ~ 15 percent!).

1.4 Implementation in time-dependent Glauber dynamics

I strongly suspect that self-correction is impossible for dynamics that obeys detailed balance, the proof likely being essentially that of Gibbs' phase rule. However, unlike

Toom's rule, squeezing dynamics is possible to induce by a rather natural form of time-dependent Glauber dynamics, viz. dynamics that obeys detailed balance with respect to a time-periodic Hamiltonian $H(t)$. This is nice because a system with a time-dependent Hamiltonian placed in contact with a (time-independent) thermal bath seems nicer from a physics perspective than dynamics driven by a overseer capable of performing L-shaped majority voting (as in Toom's rule).

To reproduce the desired squeezing of domain walls, it suffices to let $H(t)$ be an anisotropic Ising model:

$$H(t) = -J_v(t) \sum_i s_i s_{i+\hat{\mathbf{y}}} - J_h(t) \sum_i s_i s_{i+\hat{\mathbf{x}}} - h(t) \sum_i s_i \tag{15}$$

where $J_{v,h}$ and h are periodic functions of t. For simplicity we will take J_v, J_h to be positive at all times, but will (have to) allow the sign of h to change.

Consider a square minority domain of $+1$ spins. At large enough β we can make it expand horizontally faster than it expands vertically if (for example) $h > 2J_v$ but $h < 2J_h$. In this case the vertical edges of the $+$ domain will expand quickly, because each spin flip performed to expand them lowers the energy. The horizontal edges of the domain by contrast will expand slowly, with a energy-lowering process only possible after $\lfloor h/(2J_v) \rfloor > 1$ spins are flipped in a row at the domain edge. Thus if we choose

$$2J_v < h < 2J_h, \tag{16}$$

$+$ domains will for sure get fatter faster than they get taller. We thus can run Glauber dynamics with these parameters for a fixed time interval, and then switch to a set of parameters which squeeze in the opposite direction, viz. to a set of values where now

$$2J_h < -h < 2J_v. \tag{17}$$

The simplest way to do this is to simply interchange $J_v \leftrightarrow J_h$ and send $h \to -h$ at regular invervals (which amounts to periodically applying the operator $\widetilde{R}_{\pi/2}$ defined above).

In numerics, we will take a parametrization of the couplings in the form

$$H(t) = -(\bar{J} - \widetilde{J}\cos(\omega t)) \sum_i s_i s_{i+\hat{\mathbf{y}}} - (\bar{J} + \widetilde{J}\cos(\omega t)) \sum_i s_i s_{i+\hat{\mathbf{x}}} - (\bar{h} + \widetilde{h}\cos(\omega t)) \sum_i s_i. \tag{18}$$

To be concrete, we will take

$$\widetilde{J} = \frac{J}{5}, \qquad \widetilde{h} = 1, \qquad J = \frac{5}{8}, \tag{19}$$

and will let $\bar{h}$—which breaks the $\mathbb{Z}_2$ symmetry of the time-averaged Hamiltonian, and corresponds to η in the noise-based picture of the dynamics—be a tunable parameter. We will fix ω to be a constant of order J (viz. independent of L), although we may take $\omega \ll J$ without destroying the phase transition (in fact we could probably take $\omega \sim 1/\log(L)$ if desired; obviously $\omega \sim 1/L$ is too slow though).

At $\bar{h} = 0$ and $\omega = 2\pi/5$, we find relaxation times of

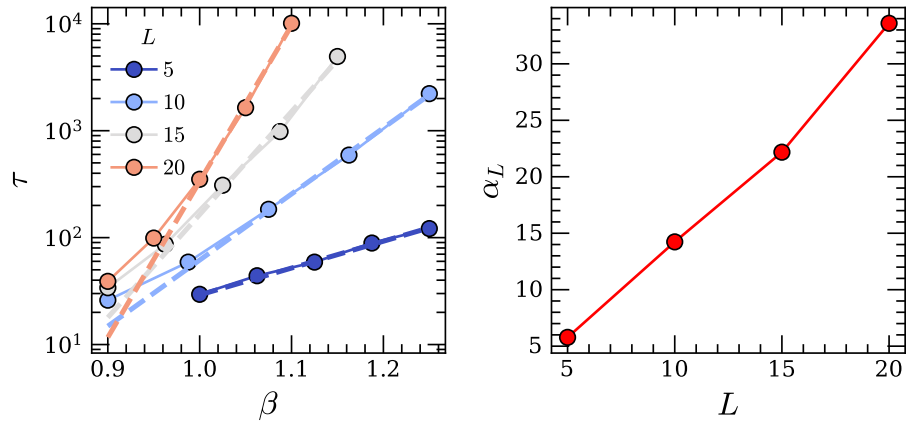

(20)

At a nonzero bias of $\bar{h} = 1/20$, we have

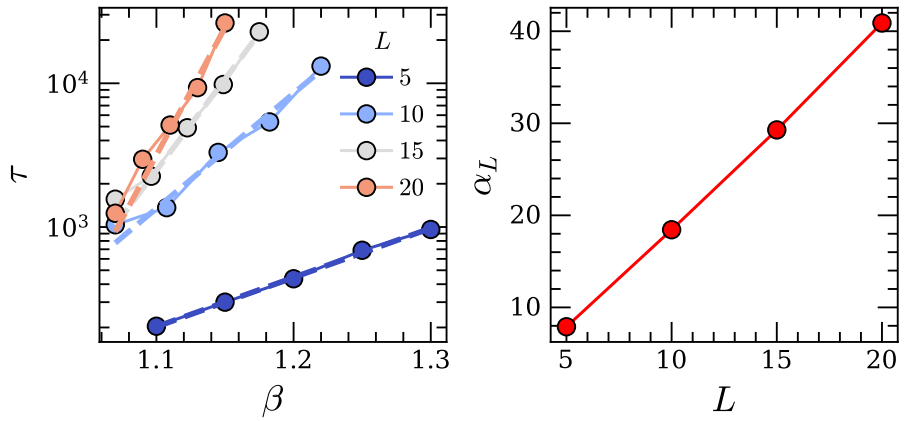

(21)

shifting the threshold β by a bit, but still giving a scaling which looks to have a converged threshold at large system sizes.

As a quick illustration of the phase diagram, consider fixing J and vary $\bar{h}$ by letting $\bar{h} = \eta\tilde{h}$ and varying η. Low-effort numerics at $\omega = 2\pi$ give

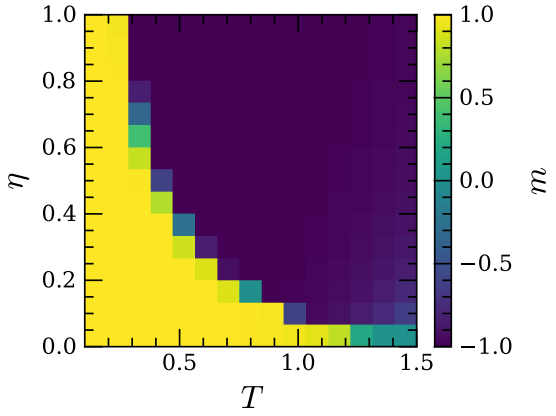

(22)

where we start in a state with $m = +1$ and bias things towards -1.

2 Mean field theory and fluctuation-stabilized order

We know from Toom's theorem that $\mathsf{S}_{2,3}$ constitute robust memories in any dimension, provided they are updated synchronously. For asynchronous updates a different calculation is required, which we turn to in this section by developing extended mean field theories that allow us to understand the error-correcting properties and phase diagrams of the asynchronously-updated $\mathsf{S}_{2,3}$ squeezing codes.

We will find that the asynchronously-updated S_2 code has a threshold in all even dimensions, provided the number of $+1$ and -1 squeezing directions are equal. However, the threshold noise strength vanishes as $p_c \propto 1/d^2$ in the $d \to \infty$ limit. This is unusual because ordering normally becomes *easier* in higher dimensions, where fluctuations are weaker. For S_3 we will find an even more dramatic result: p_c is nonzero *only* when $d = 2$.

These results owe their existence to the fact that the order which arises in these error-correcting codes is "fluctuation-stabilized", with the stability of the ordered state made possible only by spatial fluctuations in the magnetization. This fact is related to why the order dissappears in larger dimensions, since fluctuations are weaker in higher dimensions. For S_2 p_c is (roughly speaking) proportional to the strength of fluctuations, while for S_3 a critical fluctuation strength is required to maintain order, even in the absence of other noise.

2.1 Operator formalism of automaton dynamics

In the calculations to follow, we will use the Doi-Peliti operator formalism to derive dynamic mean-field equations. This formalism is slight overkill for the simplest mean field treatments (which as we will see fail for $\mathsf{S}_{2,3}$), but significantly streamlines calculations for more complicated treatments, including the cluster mean field approach adopted below.

The Doi-Peliti formalism is based on writing the evolution of the full probability distribution $P(\{s_i\})$ as a Markov equation of the form $|\partial_t P\rangle = +H|P\rangle$ for a Fock-space operator H which generates the dynamics. We will also abuse notation slightly by defining $|+\rangle$ as the un-normalized uniform sum over all configurations, so that normalization of P means $\langle +|P\rangle = 1$. Conservation of probability mandates that $|+\rangle \in \ker(H^T)$, and means that for any operator O, we may write an evolution equation for the expectation value $\langle O\rangle$ as

$$\partial_t \langle O\rangle = \langle +|[O, H]|P\rangle. \tag{23}$$

The general program adopted below will be to calculate these evolution equations for a few simple observables (such as the magnetization and short-ranged correlation functions thereof), simplifying the expectation value on the RHS using an appropriate type of mean field ansatz.

We are interested in two-state automata, and as such will write H in terms of the operators

$$a_i \equiv \frac{X_i - iY_i}{2}, \qquad n_i \equiv \frac{1 - Z_i}{2}, \qquad \bar{n}_i \equiv 1 - n_i, \tag{24}$$

which satisfy the usual

$$[n_i, a_j] = -\delta_{i,j} a_j, \qquad [n_i, a_j^\dagger] = \delta_{i,j} a_j^\dagger. \tag{25}$$

H is constructed by writing down enumerating the ways that spins can flip under the dynamics, while taking care to ensure that $\langle +|H = 0$. As a simple example, diffusion of hardcore particles on a lattice would be controlled by the Hamiltonian

$$H = \sum_{\langle i,j \rangle} (a_i^\dagger a_j - \bar{n}_i n_j), \tag{26}$$

where the second term ensures probability conservation $\langle +|H = 0$ on account of the relations

$$\langle +|a_i = \langle +|n_i, \qquad \langle +|a_i^\dagger = \langle +|\bar{n}_i. \tag{27}$$

Suppose that the noise-free automaton applies l different types of updates, each occuring with probability $q_a, a = 1, \ldots, l$ (e.g. in two dimensions $\mathsf{S}_{2,3}$ both contain two types of updates, each occuring with probability 1/2). Then in general, the noisy automata dynamics under consideration (where noise of bias η is applied with strength p) can always be formulated using the Hamiltonian

$$\begin{aligned} H = \sum_i \Bigg(& (a_i^\dagger - \bar{n}_i) \left((1-p) \sum_{a=1}^{l} q_a \Pi_i^{a,-1\to 1} + p \frac{1+\eta}{2} \right) \\ & + (a_i - n_i) \left((1-p) \sum_{a=1}^{l} q_a \Pi_i^{a,1\to -1} + p \frac{1-\eta}{2} \right) \Bigg), \end{aligned} \tag{28}$$

where $\Pi_i^{a,\pm 1 \to \mp 1}$ is a projector onto the states that would result in the spin at site i flipping from ± 1 to ∓ 1 under the action of the update rule labeled by a. For the dynamics of interest to us, these projectors will always be constructed as a polynomial in the operators n_j for j nearby i. Since we will only be interested in the dynamics of expectation values of products of the n_i, we only need calculate the commutator of H with n_i. This is easily calculated: let a given such operator be written as $O = \prod_{i \in I} n_i$ for some finite set of indices I. Letting $I_i = I \setminus \{i\}$, a short calculation gives

$$\partial_t \langle O \rangle = \sum_{i \in I} \left\langle \prod_{j \in I_i} n_j \left((1-p) \left(\sum_{a=1}^{l} \Pi_i^{a,\to 1} - n_i \right) + p \left(\frac{1+\eta}{2} - n_i \right) \right) \right\rangle. \tag{29}$$

where $\Pi_i^{a,\to 1}$ is the projector onto all states for which an application of the automaton update a would result in the spin at site i being $+1$.

Even in the simplest case where $O = n_i$, this equation is in general untractable: the RHS will involve expectation values of products of the n_j (unless each $\Pi_i^{a,\to 1} = n_{k_\alpha}$ for some site k_a, in which case the dynamics is trivial). To solve for the dynamics of $\langle n_i \rangle$ we must therefore also calculate evolution equations for multi-body products of the n_i, which in turn involve yet higher-order expectation values. This infinite regress is halted using an appropriate type of mean-field ansatz, which truncates the equations after a certain weight of operator is reached, and generates a heirachry of evolution equations which are then jointly analyzed.

Before discussing the squeezing codes—for which higher body correlation functions need to be inclued in the heirachry—we first review how mean field theory works for the simpler (and less interesting) case of Toom's rule.

2.2 Warmup: Toom's rule

First consider the case of Toom's rule in $d = 2$. The noiseless automaton possesses only a single type of update, for which a -1 spin at site i flips under the dynamics if both s_{i+x}, s_{i+y} are $+1$, and analogously for a $+1$ spin. The relevant projector is accordingly

$$\Pi_i^{\to 1} = n_i n_{i+x} + n_{i+x} n_{i+y} + n_i n_{i+y} - 2 n_i n_{i+x} n_{i+y}. \tag{30}$$

The simplest mean field ansatz assumes that correlation functions on different sites factorize:

$$\left\langle \prod_{i \in I} n_i \right\rangle \to \prod_{i \in I} \langle n_i \rangle. \tag{31}$$

Under this assumption, and re-writing things in terms of the expected magnetization

$$\langle n_i \rangle = \frac{1 + m_i}{2}, \tag{32}$$

we obtain

$$\partial_t m_i = p(\eta - m_i) + \frac{1-p}{2} \left(-m_i + m_{i+x} + m_{i+y} - m_i m_{i+x} m_{i+y} \right). \tag{33}$$

If we specify to spatially uniform configurations $m_i = m$, the mean-field equations will involve only a single variable m. In this case there is no possibility of non-reciprocity in the equations of motion, and we may always write $\partial_t m = -\delta F_{\text{eff}} / \delta m$ for some effective free energy F_{eff}. In the present setting, doing so gives

$$\partial_t m = p\eta + \frac{1-3p}{2} m - \frac{1-p}{2} m^3, \tag{34}$$

corresponding to an effective free energy of

$$F_{\text{eff}} = -p\eta m + \frac{3p-1}{4} m^2 + \frac{1-p}{8} m^4. \tag{35}$$

This free energy is bounded, and at $\eta = 0$ has an ordering transition at $p_c = 1/3$. The full phase diagram is

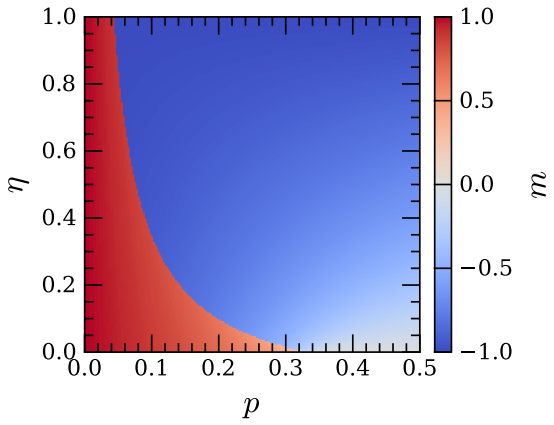

(36)

with the transition at $\eta = 0$ being second order (note: the sign of m in this plot should be flipped).

This "phase diagram" is obtained by finding the minimum of F_{eff} that is encountered by the initial state $m = -1$ as it evolves according to the above mean field equations. When $\eta > 0$, this minimum is metastable, and a solution with $m > 0$ always has lower free energy. The nontrivial statement about Toom's rule is that the lifetime of this metastable state is exponentially long (in L), but there is of course no way of assessing this statement within the context of mean field theory (the *infinite* time non-equilibrium steady state is always dominated by configurations whose magnetization agrees with that of η, so the phase diagram is only a dynamic one: the "thermodynamics" of the non-equilibrium steady states are trivial when $\eta \neq 0$). Having a mean field phase diagram like this is thus a necessary—but definitely not sufficient—condition to get a self-correcting memory. Indeed, any dynamics that proceeds by performing 3-site majority votes will yield the same phase diagram, but only votes that occur in Toom's L-shaped geometry will produce an extensively long lifetime for the metastable state.

We now briefly comment on the critical point at $\eta = 0$. The most recent numerical work studying this critical point appears to be [6]; see also [7] and the original study [1]. The conclusion of these works is that the exponents obtained for *asynchrnous* updates are the same as in the 2D Ising model, viz. $\beta \approx 0.13$, $\nu = 1$, $\gamma \approx 1.8$. For synchronous updates the exponents are different ($\beta \approx 0.11$, $\nu \approx 0.9, \gamma \approx 1.5$), but the ratios $\beta/\nu, \gamma/\nu$ are equal to the Ising values. Provided hyperscaling holds in this non-equilibrium setting (it should since the detailed balance violating terms are irrelevant), this means that the anomalous dimension η will also match the Ising value of $1/4$.

The fact that asynchronous updates yield an Ising CFT can be understood by showing that all the non-equilibrium aspects of the problem—which only appear when spatial fluctuations of m are included in the free energy—yield terms in the Langevin equation which are *irrelevant* under RG (at least within the context of the ε expansion in the dynamic RG formalism). This observation was first made in the nice paper [2]; a more detailed analysis will be given later.

2.3 S_2

We will consider a slightly general setup in which $\wedge$ squeezing (-1 expansion) occurs along the first $(d-r)/2$ spatial directions, and $\vee$ squeezing ($+1$ expansion) occurs along the remaining $(d+r)/2$ directions, with each direction of update occuring with equal probability $q_a = 1/d$, $a = 1, \ldots, d$. This dynamics possesses a $\mathbb{Z}_2$ symmetry generated by a spin flip and a reflection only when d is even and $r = 0$, and we will see momentarily that order is possible only when this symmetry is present.

The projectors in question are

$$\Pi_i^{a,\to 1} = \begin{cases} n_{i+a} n_{i-a} & a \leq \dfrac{d-r}{2} \\ 1 - \bar{n}_{i-a} \bar{n}_{i+a} & a > \dfrac{d-r}{2} \end{cases} \tag{37}$$

For any integer $l > 0$, define the "domain wall" operators

$$\begin{aligned} d_i^{la} &\equiv n_i n_{i+la} \\ \bar{d}_i^{la} &\equiv \bar{n}_i \bar{n}_{i+la} \end{aligned} \tag{38}$$

and define

$$D_i \equiv \sum_{a=1}^{(d-r)/2} d_i^{2a} - \sum_{a=(d-r)/2+1}^{d} \bar{d}_i^{2a}. \tag{39}$$

Then the time evolution of a generic product of n_i operators is given by

$$\partial_t \langle O \rangle = \sum_{i \in I} \left\langle \prod_{j \in I_i} \left(p \left(\frac{1+\eta}{2} - n_i \right) + \frac{1-p}{d} \left(\frac{d+r}{2} - d n_i + D_i \right) \right) \right\rangle \tag{40}$$

2.3.1 Fluctuationless mean field

Let us first examine the fluctuationless limit, where we take all connected correlation functions of n_i to vanish. We will furthermore assume that the expectation value of n_i is translation invariant, as keeping track of spatial derivatives in the mean field equations will not be important for any of the main points to follow. With these assumptions we have

$$\langle D \rangle = (d+r) \left(\langle n \rangle - \frac{1}{2} \right) - r \langle n \rangle^2, \tag{41}$$

and so

$$\partial_t \langle n \rangle = p \left(\frac{1+\eta}{2} - \langle n \rangle \right) + \frac{1-p}{d} r \langle n \rangle (1 - \langle n \rangle). \tag{42}$$

We will usually find it more intuitive to write our final evolution equations in terms of the magnetization

$$m_i = 2 n_i - 1, \tag{43}$$

for which (omitting the $\langle\,\rangle$s)

$$\partial_t m = p(\eta_{\text{eff}} - m) - r \frac{1-p}{2d} m^2 \tag{44}$$

where the effective bias is $\eta_{\text{eff}} = \eta + \frac{1-p}{2dp} r$. This evolution equation corresponds to an effective free energy of

$$F_{\text{eff}} = -p \eta_{\text{eff}} m + \frac{p}{2} m^2 + r \frac{1-p}{6d} m^3. \tag{45}$$

There are a few things to take away from this. First, consider the symmetric case where d is even and $r = 0$. We then get the extremely simple

$$\partial_t m = p(\eta - m), \tag{46}$$

which is the evolution equation we would get in the presence of noise alone: m simply relaxes to the average value η of the noise over a timescale $1/p$. Thus the effects of the error-correction being performed by the S_2 automaton do not even appear when

fluctuations of the magnetization are neglected, and there is clearly no possibility of having an ordered phase in this limit. It is of course possible for the presence of fluctuations to change this conclusion, but since fluctuations enter only at an order of at most $1/d$, the critical noise strength must vanish with d at least as fast as $p_c \sim 1/d$ (we will see that in fact $p_c \sim 1/d^2$).

Secondly, when $r \neq 0$, the absence of symmetry is reflected in both the modification of η, and in the generation of an m^3 term in the effective free energy. This gives a free energy with only one local minimum (the other extremal point is a local maximum), which is not compatible with the existence of a stable memory. Furthermore, the size of both the induced bias and the m^2 term appearing in $\partial_t m$ are $O(1)$ as $p \to 0$. Thus our conlcusion about the absence of two stable fixed points for m in the range $[-1, 1]$ will remain true beyond the present mean field approximation as long as d is large enough. This means that there can be no order in large enough d with asynchronous updates if $r \neq 0$, viz. if the $\mathbb{Z}_2$ symmetry is not present. We will later numerically check that in fact $p_c = 0$ when $d = 3$: thus with asynchronous updates, S_2 can only order when $d \in 2\mathbb{Z}$ and $r = 0$. We will accordingly specify to this case in the remainder of this subsection.

2.3.2 Adding fluctuations

Assuming that the symmetries that permute among the first $d/2$ dimensions and the last $d/2$ are not spontaneously broken (this statement is vacuous when $d = 2$, and when $d > 2$ it is numerically observed to be true), we may write

$$\frac{\langle D \rangle}{d} = \frac{\langle d^{2x} \rangle - \langle \bar{d}^{2y} \rangle}{2}, \tag{47}$$

where x is one of the first $d/2$ coordinates, and y is one of the last $d/2$. The exact evolution equation for $\langle n \rangle$ is then

$$\partial_t \langle n \rangle = \frac{1}{2} \left(1 + \eta p - 2\langle n \rangle + (1-p)(\langle d^{2x} \rangle - \langle \bar{d}^{2y} \rangle) \right). \tag{48}$$

We thus need to solve for the as-yet unknown expectation values $\langle d^{2x} \rangle, \langle \bar{d}^{2y} \rangle$. A straightforward calculation gives

$$\partial_t \langle d^{la} \rangle = (1 + \eta p)\langle n \rangle - 2\langle d^{la} \rangle + 2\frac{1-p}{d} \langle n_j D_{j+la} \rangle \tag{49}$$

where we have used $\langle n_j D_{j+la} \rangle = \langle n_{j+la} D_j \rangle$.[5] By symmetry, we similarly obtain

$$\partial_t \langle \bar{d}^{la} \rangle = (1 - \eta p)\langle \bar{n} \rangle - 2\langle \bar{d}^{la} \rangle - 2\frac{1-p}{d} \langle \bar{n}_j D_{j+la} \rangle. \tag{50}$$

Again under these assumptions, we have

$$\langle n_j D_{j+2a} \rangle = \langle n_j n_{j+x} n_{j+3x} \rangle + (d/2-1)\langle n_j n_{j+2x-w} n_{j+2x+w} \rangle - \frac{d}{2} \langle n_j \bar{n}_{j+2x-y} \bar{n}_{j+2x+y} \rangle \qquad (a \leq d/2) \tag{51}$$

[5] Translation implies $\langle n_{j+la} D_j \rangle = \langle n_j D_{j-la} \rangle$ and then $\langle d^{la} \rangle = \langle d^{-la} \rangle$.

and

$$\langle \bar{n}_j D_{j+2a} \rangle = -\langle \bar{n}_j \bar{n}_{j+y} \bar{n}_{j+3y} \rangle - (d/2-1)\langle \bar{n}_j \bar{n}_{j+2y-z} \bar{n}_{j+2y+z} \rangle + \frac{d}{2}\langle \bar{n}_j n_{j+2x-y} n_{j+2x+y} \rangle \qquad (a > d/2) \tag{52}$$

where $w \neq x$ is an arbitrary coordinate with $w \leq d/2$ and $z \neq y$ is a coordinate with $z > d/2$.

We will truncate the heirarchy of cluster mean-field equations by only keeping correlations between nearest-neighbors and those next-nearest-neighbors which are of the form $(i, i \pm 2a)$ for some a (thus for example we do not keep correlations between nnn pairs like $(i, i+a+b)$ for $a \neq b$—this choice keeps the minimal number of variables needed to get an ordered phase). This means that we take e.g.

$$\langle n_j n_{j+2a-b} n_{j+2a+b} \rangle \to \langle n \rangle \langle d^{2b} \rangle \tag{53}$$

and[6]

$$\langle n_j n_{j+a} n_{j+3a} \rangle \to \frac{\langle d^{1a} \rangle \langle d^{2a} \rangle}{\langle n \rangle}. \tag{54}$$

Therefore

$$\langle n_j D_{j+2a} \rangle = \frac{\langle d^{1x} \rangle \langle d^{2x} \rangle}{\langle n \rangle} + (d/2-1)\langle n \rangle \langle d^{2x} \rangle - \frac{d}{2}\langle n \rangle \langle \bar{d}^{2y} \rangle \qquad (a \leq d/2) \tag{55}$$

and

$$\langle \bar{n}_j D_{j+2a} \rangle = -\frac{\langle \bar{d}^{1y} \rangle \langle \bar{d}^{2y} \rangle}{\langle \bar{n} \rangle} - (d/2-1)\langle \bar{n} \rangle \langle \bar{d}^{2y} \rangle + \frac{d}{2}\langle \bar{n} \rangle \langle d^{2x} \rangle \qquad (a > d/2). \tag{56}$$

Similarly,

$$\langle n_j D_{j+a} \rangle = \langle d^{2x} \rangle (1 - \langle n \rangle) + \frac{d}{2}\langle n \rangle (\langle d^{2x} \rangle - \langle \bar{d}^{2y} \rangle) \qquad (a \leq d/2) \tag{57}$$

and

$$\langle \bar{n}_j D_{j+a} \rangle = -\langle \bar{d}^{2y} \rangle (1 - \langle \bar{n} \rangle) + \frac{d}{2}\langle \bar{n} \rangle (\langle d^{2x} \rangle - \langle \bar{d}^{2y} \rangle) \qquad (a > d/2) \tag{58}$$

where we used relations like $n_j^2 = n_j$ and $\langle n_j n_{j+a-b} n_{j+a+b} \rangle \to \langle n \rangle \langle d^{2b} \rangle$ for $a \neq b$ (the latter following from our neglect of diagonal nnn correlations).

[6] This follows from $P(n_j n_{j+a} n_{j+3a}) = P(n_j | n_{j+a} n_{j+3a}) P(n_{j+a} n_{j+3a}) = P(n_j | n_{j+a}) P(n_{j+a} n_{j+3a}) = P(n_j n_{j+a}) P(n_{j+a} n_{j+3a}) / P(n_{j+a}) = \langle d^{1a} \rangle \langle d^{2a} \rangle / \langle n \rangle$, where $P(\Pi_{i \in I} n_i)$ is the probability of finding $n_i = +1$ at all sites in the set I, and our factorization assumption enters in the second equality.

Collecting results, our cluster mean field equations read

$$\begin{aligned}
\partial_t\langle n\rangle &= \frac{1}{2}\left(1+\eta p - 2\langle n\rangle + (1-p)(\langle d^{2x}\rangle - \langle \bar{d}^{2y}\rangle)\right)\\
\partial_t\langle d^{1x}\rangle &= (1+\eta p)\langle n\rangle - 2\langle d^{1x}\rangle + 2\frac{1-p}{d}\left(\langle d^{2x}\rangle\langle \bar{n}\rangle + \frac{d}{2}\langle n\rangle(\langle d^{2x}\rangle - \langle \bar{d}^{2y}\rangle)\right)\\
\partial_t\langle \bar{d}^{1y}\rangle &= (1-\eta p)\langle \bar{n}\rangle - 2\langle \bar{d}^{1y}\rangle - 2\frac{1-p}{d}\left(-\langle \bar{d}^{2y}\rangle\langle n\rangle + \frac{d}{2}\langle \bar{n}\rangle(\langle d^{2x}\rangle - \langle \bar{d}^{2y}\rangle)\right)\\
\partial_t\langle d^{2x}\rangle &= (1+\eta p)\langle n\rangle - 2\langle d^{2x}\rangle + 2\frac{1-p}{d}\left(\langle d^{2x}\rangle\left(\frac{\langle d^{1x}\rangle}{\langle n\rangle} - \langle n\rangle\right) + \frac{d}{2}\langle n\rangle(\langle d^{2x}\rangle - \langle \bar{d}^{2y}\rangle)\right)\\
\partial_t\langle \bar{d}^{2y}\rangle &= (1-\eta p)\langle \bar{n}\rangle - 2\langle \bar{d}^{2y}\rangle - 2\frac{1-p}{d}\left(-\langle \bar{d}^{2y}\rangle\left(\frac{\langle \bar{d}^{1y}\rangle}{\langle \bar{n}\rangle} - \langle \bar{n}\rangle\right) + \frac{d}{2}\langle \bar{n}\rangle(\langle d^{2x}\rangle - \langle \bar{d}^{2y}\rangle)\right)
\end{aligned} \tag{59}$$

It will be more useful to write these equations in terms of variables that transform in definite representations of the $\mathbb{Z}_2$ symmetry, viz. the magnetization and the linear combinations

$$d^{l\pm} \equiv \frac{d^{lx} \pm \bar{d}^{ly}}{2}. \tag{60}$$

d^{l+} is neutral under the $\mathbb{Z}_2$ symmetry, while d^{l-} transforms in the same way as m. Some agebra turns the MF equations into (omitting $\langle\,\rangle$s)

$$\begin{aligned}
\partial_t m &= p\eta - m + 2(1-p)d^{2-}\\
\partial_t d^{1+} &= \frac{1+\eta p m}{2} - 2d^{1+} + \frac{1-p}{d}\left(d^{2+} + (d-1)md^{2-}\right)\\
\partial_t d^{1-} &= \frac{\eta p + m}{2} - 2d^{1-} + \frac{1-p}{d}\left(-md^{2+} + (1+d)d^{2-}\right)\\
\partial_t d^{2+} &= \frac{1+\eta p m}{2} - 2d^{2+} + 4\frac{1-p}{d(1-m^2)}\left(d^{2+}d^{1+} + d^{2-}d^{1-} - m(d^{2+}d^{1-} + d^{2-}d^{1+})\right)\\
&\quad + \frac{1-p}{d}\left((d-1)md^{2-} - d^{2+}\right)\\
\partial_t d^{2-} &= \frac{m+\eta p}{2} - 2d^{2-} + 4\frac{1-p}{d(1-m^2)}\left(d^{1+}d^{2-} + d^{1-}d^{2+} - m(d^{2+}d^{1+} + d^{2-}d^{1-})\right)\\
&\quad + \frac{1-p}{d}\left((d-1)d^{2-} - md^{2+}\right)
\end{aligned} \tag{61}$$

Things become a bit nicer still if we write things not in terms of the $d^{l\pm}$, but rather in terms of the connected correlation functions of the magnetization. Define the correlation functions

$$f_i^{la} \equiv \langle m_i m_{i+la}\rangle - \langle m_i\rangle\langle m_{i+la}\rangle, \tag{62}$$

together with their linear combinations

$$f^{l\pm} \equiv \frac{f^{lx} \pm f^{ly}}{2}. \tag{63}$$

The $f^{l\pm}$ will vanish both at $p = 0$ and $p = 1$, where the system has no nontrivial spatial correlations. A short calculation gives the following relations between $d^{l\pm}$ and

$f^{l\pm}$: (again assuming translation invariance and dropping spatial indices)

$$\begin{aligned}\langle d^{l+}\rangle &= \frac{1}{4}(f^{l+} + 1 + m^2)\\ \langle d^{l-}\rangle &= \frac{1}{4}(f^{l-} + 2m).\end{aligned} \tag{64}$$

Substituting this in our previous MF equations yields, after some thankless algebra,

$$\begin{aligned}\partial_t m &= p(\eta - m) + \frac{1-p}{2} f^{2-}\\ \partial_t f^{1-} &= -2f^{1-} + \frac{1-p}{d}\left(m(1-m^2) + f^{2-} - m f^{2+}\right)\\ \partial_t f^{2-} &= -2f^{2-} + \frac{1-p}{d}\left(f^{1-} + m f^{1+} + \frac{1}{1-m^2}\left(f^{1-}f^{2+} + f^{1+}f^{2-} - m(f^{1-}f^{2-} + f^{1+}f^{2+})\right)\right)\\ \partial_t f^{1+} &= -2f^{1+} + \frac{1-p}{d}\left(1 - m^2 + f^{2+} - m f^{2-}\right)\\ \partial_t f^{2+} &= -2f^{2+} + \frac{1-p}{d}\left(f^{1+} + m f^{1-} + \frac{1}{1-m^2}\left(f^{1+}f^{2+} + f^{1-}f^{2-} - m(f^{1+}f^{2-} + f^{1-}f^{2+})\right)\right)\end{aligned} \tag{65}$$

The trivial disordered state, which has $m = f^{1-} = f^{2-} = 0$, is easily seen to have $\mathbb{Z}_2$-invariant fluctuations of size

$$f^{1+} = \sqrt{f^{2+}} = \frac{1 - \sqrt{1-\zeta^2}}{\zeta}, \tag{66}$$

where we have defined

$$\zeta \equiv \frac{1-p}{d}. \tag{67}$$

In the $d \to \infty$ limit we have

$$f^{1+} = \frac{1-p}{2d} + O(1/d^2), \tag{68}$$

so that $f^{1+} \sim 1/d$ and $f^{2+} \sim 1/d^2$ to leading order, consistent with fluctuations being suppressed as $1/d$ (this is essentially just a consequence of the central limit theorem).

In the ordered state, one may similarly verify the scalings $m \sim d^0$, $f^{1-} \sim 1/d$, and $f^{2-} \sim 1/d^2$. From this scaling and the equation for $\partial_t m$, we thus conclude that $p_c \sim 1/d^2$. Indeed, one can find p_c analytically by linearizing the mean field equations about the disordered state, and then determining the point at which the disordered solution becomes unstable. The details involve some fairly tedious algebra and will be skipped; here we quote only the result

$$p_c = \frac{1}{1+4d^2}. \tag{69}$$

In 2d, this predicts $p_c = 1/17 \approx 0.058$, which is about a factor of 2 larger than the value observed numerically.

The phase diagram in $d = 2$ one obtains from these equations gives a magnetization which (unsurprisingly) looks like

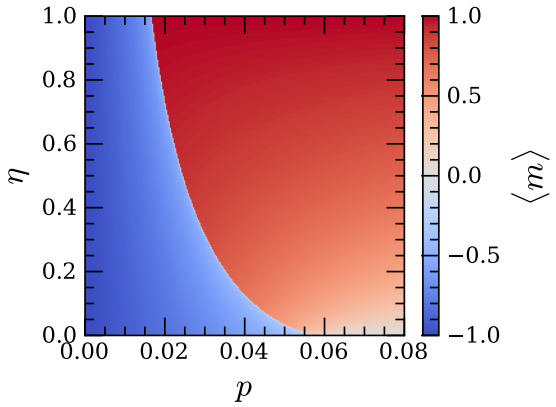

(70)

We may also look at the connected correlation functions $f^{l\pm}$. The charge-neutral flutuations f^{1+} look like

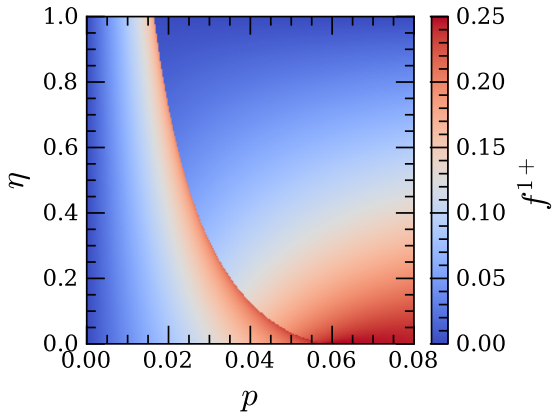

(71)

while the charged fluctuations f^{1-} are

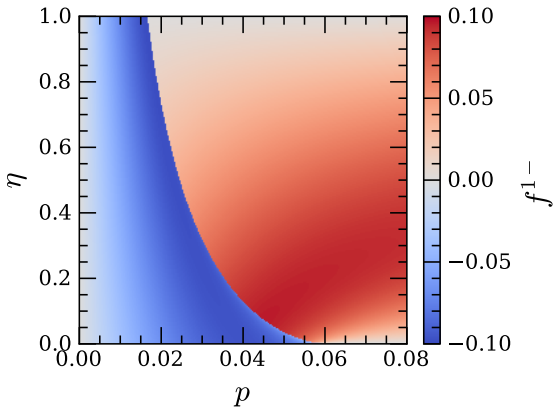

(72)

2.4 S_3

We now consider the three-variable rule S_3 (6), which as we will see has rather different physics. Like S_2, similar arguments show that S_3 is disordered under asynchronous updates in all cases where a $\mathbb{Z}_2$ symmetry is not present. For this reason we will continue

to specify to even dimensions, with the number of $\wedge$ and $\vee$ squeezing directions both equal to $d/2$.

The relevant projector that determines the dynamics is now cubic in the number operators:

$$\Pi_i^{a,\to 1} = \begin{cases} n_{i+a} n_i n_{i-a} & a \leq \dfrac{d}{2} \\ 1 - \bar{n}_{i-a} \bar{n}_i \bar{n}_{i+a} & a > \dfrac{d}{2} \end{cases}. \tag{73}$$

Define the operators

$$D_i^1 \equiv \sum_{a=1}^{d/2} d_i^{2a}, \qquad D_i^2 \equiv \sum_{a=d/2+1}^{d} \bar{d}_i^{2a}. \tag{74}$$

Then a generic product of number operators evolves as

$$\partial_t \langle O \rangle = \sum_{i \in I} \left\langle \prod_{j \in I_i} \left(p \left(\frac{1+\eta}{2} - n_i \right) + (1-p) \left(\frac{1}{2} - n_i + \frac{1}{d} (n_i D_i^1 - \bar{n}_i D_i^2) \right) \right) \right\rangle. \tag{75}$$

2.4.1 Fluctuationless mean field

We begin by looking at the limit in which all correlation functions factorize and are translation invariant. In this limit, we have

$$\frac{1}{d} \langle n_i D_i^1 - \bar{n}_i D_i^2 \rangle = \frac{1}{8} (3m + m^3). \tag{76}$$

We then find

$$\partial_t m = p\eta - \frac{1+3p}{4} m + \frac{1-p}{4} m^3 \tag{77}$$

which corresponds to a free energy of

$$F_{\text{eff}} = -p\eta m + \frac{1+3p}{8} m^2 - \frac{1-p}{16} m^4. \tag{78}$$

The most important thing to note about this free energy is that it is not compatible with the existence of an ordered phase: for all values of p, the disordered fixed point is always stable, and the ordered fixed points are always unstable. Therefore like S_2, no ordering is possible within mean field theory. Unlike S_2 though, fluctuation corrections to this result cannot produce order once d is large enough, since in the present case the mass term in F_{eff} is positive and non-vanishing in the limit $p \to 0$. Thus there must be a critical dimension d_c such that the system is disordered for *all* p as long as $d > d_c$. Numerically (as well as within the following mean field analysis) zthis dimension turns out to be $d_c = 2$, so that S_3 with asynchronous updates orders *only* in two dimensions.

2.4.2 Adding fluctuations

The expectation values $\langle n_j D_j^1 \rangle, \langle \bar{n}_j D_j^2 \rangle$ on the RHS involve sums of operators of the form $\langle n_i n_{i+a} n_{i+2a} \rangle$. Since these do not factorize even when only *nearest* neighbors are taken into account, we wil make our life easier by doing an extended cluster mean field

theory involving only the d^{1a}, taking correlation functions of the n_j to factorize beyond nearest neighbors (for S_2 we were forced to account for nnn correlations since $\partial_t\langle n\rangle$ would otherwise trivially lead to $\langle n\rangle = (1+\eta)/2$). In this scheme, and working with the assumption that translation and the relevant reflection symmetries are unbroken, we have

$$\langle n_j D_j^1\rangle = \sum_{a=1}^{d/2} \frac{\langle d_{j-a}^{1a}\rangle\langle d_j^{1a}\rangle}{\langle n_j\rangle}, \qquad \langle \bar{n}_j D_j^2\rangle = \sum_{b=d/2+1}^{d} \frac{\langle \bar{d}_{i-b}^{1b}\rangle\langle \bar{d}_i^{1b}\rangle}{\langle \bar{n}_j\rangle}. \tag{79}$$

We then just need the evolution equations for $\langle d_j^{1a}\rangle$. These are (here as before x is any coordinate less than $d/2+1$, and y is any coordinate greater than $d/2$)

$$\begin{aligned}
\partial_t\langle d_j^{1x}\rangle &= \frac{1+\eta p}{2}\langle n_j + n_{j+x}\rangle - 2\langle d_j^{1x}\rangle + \frac{1-p}{d}\left(\langle d_j^{1x}(D_{j+x}^1 + D_j^1)\rangle - \langle n_j\bar{n}_{j+x}D_{j+x}^2 + n_{j+x}\bar{n}_j D_j^2\rangle\right)\\
\partial_t\langle \bar{d}_j^{1y}\rangle &= \frac{1-\eta p}{2}\langle \bar{n}_j + \bar{n}_{j+y}\rangle - 2\langle \bar{d}_j^{1y}\rangle + \frac{1-p}{d}\left(\langle \bar{d}_j^{1y}(D_{j+y}^2 + D_j^2)\rangle - \langle \bar{n}_j n_{j+y}D_{j+y}^1 + \bar{n}_{j+y}n_j D_j^1\rangle\right)
\end{aligned} \tag{80}$$

For spatially uniform solutions, this simplifies to

$$\begin{aligned}
\partial_t\langle d^{1x}\rangle &= (1+\eta p)\langle n\rangle - 2\langle d^{1x}\rangle + 2\frac{1-p}{d}\langle n_{j+x}n_j D_j^1 - n_{j+x}\bar{n}_j D_j^2\rangle\\
\partial_t\langle d^{1y}\rangle &= (1-\eta p)\langle \bar{n}\rangle - 2\langle \bar{d}^{1y}\rangle - 2\frac{1-p}{d}\langle \bar{n}_j n_{j+y}D_{j+y}^1 - \bar{n}_j\bar{n}_{j+y}D_{j+y}^2\rangle.
\end{aligned} \tag{81}$$

Our factorization assumption lets us simplify the four-point functions above, giving e.g.

$$\langle d_j^{1x}(D_{j+x}^1 + D_j^1)\rangle = \langle d_j^{1x}\rangle\Delta^{1x}\left(\frac{\langle d_{j-x}^{1x}\rangle}{\langle n_j\rangle} + \sum_{b\neq a}^{d/2}\frac{\langle d_{j-b}^{1b}\rangle\langle d_j^{1b}\rangle}{\langle n_j\rangle^2}\right) \tag{82}$$

where

$$\Delta^{la}(\mathcal{O}_j) \equiv \mathcal{O}_j + \mathcal{O}_{j+la}. \tag{83}$$

We also have

$$\langle n_j\bar{n}_{j+x}D_{j+x}^2 + n_{j+x}\bar{n}_j D_j^2\rangle = \sum_{b=d/2+1}^{d}\left(\frac{(\langle n_j\rangle - \langle d_j^{1x}\rangle)\langle \bar{d}_{j+x}^{1b}\rangle\langle \bar{d}_{j-b+x}^{1b}\rangle}{\langle \bar{n}_{j+x}\rangle^2} + \frac{(\langle n_{j+x}\rangle - \langle d_j^{1x}\rangle)\langle \bar{d}_j^{1b}\rangle\langle \bar{d}_{j-b}^{1b}\rangle}{\langle \bar{n}_j\rangle^2}\right) \tag{84}$$

$$\begin{aligned}
\langle n_{j+x}n_j D_j^1\rangle &= \langle n_{j+x}n_j n_{j-x}\rangle + (d/2-1)\langle n_{j+x}n_j n_{j-w}n_{j+w}\rangle\\
&\to \frac{\langle d^{1x}\rangle^2}{\langle n\rangle} + (d/2-1)\frac{\langle d^{1x}\rangle^3}{\langle n\rangle^2}
\end{aligned} \tag{85}$$

and similarly

$$\begin{aligned}
\langle n_{j+x}\bar{n}_j D_j^2\rangle &\to \frac{d}{2}\frac{\langle \bar{d}^{1y}\rangle^2}{\langle \bar{n}\rangle^2}(\langle n\rangle - \langle d^{1x}\rangle)\\
\langle \bar{n}_j n_{j+y}D_{j+y}^1\rangle &\to \frac{d}{2}\frac{\langle d^{1x}\rangle^2}{\langle n\rangle^2}(\langle \bar{n}\rangle - \langle \bar{d}^{1y}\rangle)\\
\langle \bar{n}_j\bar{n}_{j+y}D_{j+y}^2\rangle &\to \frac{\langle \bar{d}^{1y}\rangle^2}{\langle \bar{n}\rangle} + (d/2-1)\frac{\langle \bar{d}^{1y}\rangle^3}{\langle \bar{n}\rangle^2}.
\end{aligned} \tag{86}$$

Recapitulating, the mean field equations are

$$\begin{aligned}
\partial_t\langle n\rangle &= \frac{1+\eta p}{2} - \langle n\rangle + \frac{1-p}{2}\left(\frac{\langle d^{1x}\rangle^2}{\langle n\rangle} - \frac{\langle \bar{d}^{1y}\rangle^2}{\langle \bar{n}\rangle}\right)\\
\partial_t\langle d^{1x}\rangle &= (1+\eta p)\langle n\rangle - 2\langle d^{1x}\rangle + (1-p)\left(\frac{\langle d^{1x}\rangle^2}{\langle n\rangle}\left(\frac{2}{d} + \left(1-\frac{2}{d}\right)\frac{\langle d^{1x}\rangle}{\langle n\rangle}\right) - \frac{\langle \bar{d}^{1y}\rangle^2}{\langle \bar{n}\rangle^2}(\langle n\rangle - \langle d^{1x}\rangle)\right)\\
\partial_t\langle \bar{d}^{1y}\rangle &= (1-\eta p)\langle \bar{n}\rangle - 2\langle \bar{d}^{1y}\rangle + (1-p)\left(\frac{\langle \bar{d}^{1y}\rangle^2}{\langle \bar{n}\rangle}\left(\frac{2}{d} + \left(1-\frac{2}{d}\right)\frac{\langle \bar{d}^{1y}\rangle}{\langle \bar{n}\rangle}\right) - \frac{\langle d^{1x}\rangle^2}{\langle n\rangle^2}(\langle \bar{n}\rangle - \langle \bar{d}^{1y}\rangle)\right)
\end{aligned} \tag{87}$$

Written in terms of variables $m, d^{\pm}$ which have definite charges under the $\mathbb{Z}_2$ symmetry, this becomes

$$\begin{aligned}
\partial_t m &= \eta p - m + \frac{4(1-p)}{1-m^2}\left(2d^+d^- - m((d^+)^2 + (d^-)^2)\right)\\
\partial_t d^+ &= \frac{1+\eta p m}{2} - 2d^+\\
&\quad + 2\frac{1-p}{(1-m^2)^2}\Big(((d^+)^2 + (d^-)^2)\left(-1 + 2/d - (3+2/d)m^2 + 4(1-1/d)(1+m^2)d^+ + (8/d)md^-\right)\Big)\\
&\quad + 2d^+d^-\left((3-2/d)m + (2/d+1)m^3 - 4/d(1+m^2)d^- - 8(1-1/d)md^+\right)\\
\partial_t d^- &= \frac{m+\eta p}{2} - 2d^-\\
&\quad + 2\frac{1-p}{(1-m^2)^2}\Big(((d^+)^2 + (d^-)^2)\left(-(3+2/d)m - (1-2/d)m^3 + 4(1-1/d)(1+m^2)d^- + (8/d)md^+\right)\\
&\quad + 2d^+d^-\left(1 + 2/d + (3-2/d)m^2 - 4/d(1+m^2)d^+ - 8(1-1/d)md^-\right)\Big)
\end{aligned} \tag{88}$$

Finally, switching from $d^{\pm}$ to the connected correlation functions $f^{\pm}$ of the magnetization, a henious amount of algebra produces

$$\begin{aligned}
\partial_t m &= \eta p - \frac{1+3p}{4}m + \frac{1-p}{4}m^3 + \frac{1-p}{4}\left(\frac{2f^+f^- - m((f^+)^2 + (f^-)^2)}{1-m^2} + 2(mf^+ + f^-)\right)\\
\partial_t f^- &= -2f^- + \frac{1-p}{2d}\Big(2m(1-m^2) + (1+d+(d-3)m^2)f^- - 2f^+m + 2df^-f^+\\
&\quad - \frac{1}{1-m^2}\left(2m((f^-)^2 + (f^+)^2) + 2(1-3m^2)f^+f^-\right)\\
&\quad + \frac{1}{(1-m^2)^2}\big(2m(f^+)^3 - 2(2d-3)m(f^-)^2f^+ + (d-3)(1+m^2)f^-(f^+)^2\\
&\quad + (d-1)(1+m^2)(f^-)^3\big)\Big)\\
\partial_t f^+ &= -2f^+ + \frac{1-p}{2d}\Big(1 - m^4 + (1+d+(d-3)m^2)f^+ - 2f^-m + 2d(f^+)^2\\
&\quad - \frac{1}{1-m^2}\left(4mf^-f^+ + (1-3m^2)((f^+)^2 + (f^-)^2)\right)\\
&\quad + \frac{1}{(1-m^2)^2}\big(2m(f^-)^3 - 2(2d-3)mf^-(f^+)^2 + (d-3)(1+m^2)(f^-)^2f^+\\
&\quad + (d-1)(1+m^2)(f^+)^3\big)\Big).
\end{aligned} \tag{89}$$

ethan: *one kind of annoying thing is that the ordered fixed point at $p \to 0$ can only be obtained by cancelling the vanishing of $f^{\pm}$ in the numerator by the vanishing of $1 - m^2$ in the denomenator…* The existence of an ordered phase is most easily established by examining the stability of the disordered fixed point. ethan: *this argument only shows that spontaneous symmetry breaking is impossible when d is large enough. I also need to rule out a situation where stable disordered and ordered fixed points are simultaneously present…* We can show that an ordered phase does not exist when d is made large enough by showing that the disordered fixed point remains stable for all p when d is sufficiently large. To this end, we first solve $\partial_t f^+ = 0$ in the $d \to \infty$ limit. This is done by expanding f^+ as a series in $1/d$. The leading $O(1)$ part is easiliy checked to vanish[7] (as it should, on account of fluctuations vanishing as $d \to \infty$), while the leading $1/d$ part gives an equation that is easily solved to produce

$$f^+ = \frac{1-p}{d(3+p)} + O(1/d^2). \tag{90}$$

The mass matrix $M^{ab} = -\delta\partial_t\phi^a/\delta\phi^b$ for $\phi = (m, f^-)$ is

$$M = \begin{pmatrix} \frac{1+3p}{4} - \frac{1-p}{4} f^+(2-f^+) & -\frac{1-p}{2}(1+f^+) \\ \frac{1-p}{d}(-(f^+)^3 + (f^+)^2 + f^+ - 1) & 2 - \frac{1-p}{2d}((f^+)^2(d-3) + 2(d-1)f^+ + d + 1) \end{pmatrix}, \tag{91}$$

which is allowed to be not-symmetric by virtue of the non-equilibrium nature of the present problem. Since $f^+ \sim 1/d$, we have

$$M|_{d\to\infty} = \begin{pmatrix} \frac{1+3p}{4} & -\frac{1-p}{2} \\ 0 & \frac{3+p}{2} \end{pmatrix} + O(1/d). \tag{92}$$

Both eigenvalues of M are thus positive and $O(1)$ even when $p = 0$, provided d is large enough. This shows that the model is always disordered for $d > d_c$, with finite d_c. In the present mean field analysis it turns out that $d_c = 2$, which agrees with the critical dimension seen in numerics.

To see this graphically, the magnetization in $d = 2$ has a typical-looking phase diagram (with a value of p_c correspondingly smaller than that of S_2):

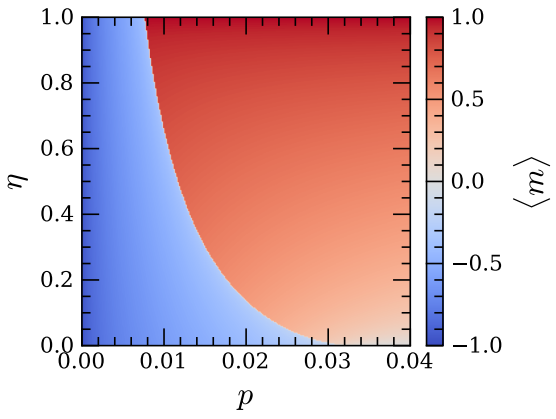

(93)

[7] The equation for the $O(1)$ part is solved either by $f^+ = 0$ or by $f^+ = \frac{2}{\sqrt{1-p}} - 1$. This latter solution is unphysical, since f^+ is bounded from above by 1.

The fluctuations of the magnetization have the same qualitative behavior as for S_2. Unlike S_2 however, there is no ordered phase above $d = 2$: for $d = 4$, the magnetization is simply

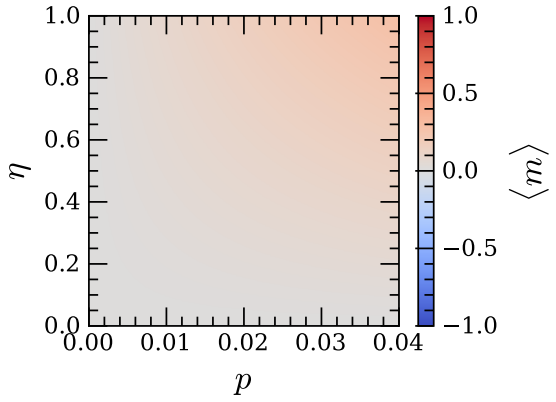

(94)

2.4.3 Proof that no equilibrium description exists

We have seen in S_3 an example of a theory where, when fluctuations in m are ignored, one obtains an unstable effective free energy $F_{\text{eff}}[m]$ incompatible with the existence of an ordered phase. In this subsection we show that a situation like this cannot occur for any dynamics that obeys detailed balance (that is, any dynamics whose Langevin equation is obtained by differentiating a free energy). A priori one might imagine that the sickness in $F_{\text{eff}}[m]$ could be cured by adding in additional fields $\phi^2, \phi^3, \ldots$ that couple to m in some way, but the above statement means that this is not possible.

The proof is rather trivial. Consider a theory with field variables ϕ^a, where a is some arbitrary index and $\phi^1 = m$ is the magnetization. Without loss of generality, the $\phi^{a>1}$ can be taken to correspond to connected correlation functions involving the m variables, which vanish in the $d \to \infty$ limit where correlation functions factorize.

As above, define the mass matrix

$$M^{ab}_{\phi_*} \equiv -\frac{\delta \partial_t \phi^a}{\delta \phi^b}\Big|_{\phi_*}, \tag{95}$$

where ϕ_* is a particular fixed point. The fixed point is stable only if all of the eigenvalues of M_{ϕ_*} are positive.

Consider a situation where the $d \to \infty$ limit gives an unstable solution for the magnetization. This means that when we set $\phi^{a>1} = 0$, the $m \neq 0$ solution(s) of the mean field equations are unstable. This statement is equivalent to $M^{11}_{\phi_*} < 0$.

As we have seen above, adding additional fields $\phi^{a>1}$ *can* stabilize the fixed point, even when $\phi^{a>1}_* = 0$. However, if the dynamics obeys detailed balance, the instability remains. Indeed, if we are describing the dynamics with an effective free energy, M must be a symmetric matrix. The assumption that all of M's eigenvalues are positive—which means M is positive-definite, by symmetry—is then in contradiction with the fact that $\langle e_1|M|e_1\rangle = M^{11} < 0$ (where $\langle a|e_1\rangle = \delta_{a,1}$). Therefore ϕ_* cannot be a stable fixed point if the dynamics is described by an effective free energy.

3 Coarsening dynamics

In this section we will examine how coarsening occurs in the ordered phase. On general grounds we expect the coarsening of the magnetiation m to be described by a Langevin equation of the form

$$\partial_t m = K\nabla^2 m + \widetilde{K}_a(\partial_a m)^2 - V'(m) - \bar{h} \tag{96}$$

where $V' = \delta V/\delta m$ is the gradient of an appropriate potential (e.g. $V(m) = \frac{1}{4}(1 - m^2)^2$), and the KPZ-like interaction strengths $\widetilde{K}_a$ are positive along some subset of the spatial directions, and negative along the remaining directions. It is easy to show that as long as the $\widetilde{K}_a$ are not all equal, this equation cannot be the result of differentiating a free energy.

In this section we will first see why (96) leads to squeezing-type coarsening dynamics, and will then derive (96) in the context of the time-dependent Glauber dynamics implementation.

3.1 Domain wall dynamics

3.1.1 one dimension

In order to see why the KPZ-like nonlinearities induce ballistic motion of minority domains in the ordered state let us first consider what happens in 1d, where we have simply a KPZ equation modified by the $V'(m)$ interaction:

$$\partial_t m = K\partial_x^2 m + \widetilde{K}(\partial_x m)^2 - V'(m) - \bar{h}. \tag{97}$$

Consider a configuration where m changes monotonically from ± 1 at $x = -\infty$ to ∓ 1 at $x = +\infty$. We claim that no such configuration can be a static solution to this PDE if $\bar{h}$ or $\widetilde{K}$ are nonzero. Indeed, setting $\partial_t m = 0$, multiplying both sides by $\partial_x m$, and integrating over all of space, we have

$$\begin{aligned}
\widetilde{K}\int_{\mathbb{R}}(\partial_x m)^3 &= \int_{\mathbb{R}}\left(-K\partial_x m\partial_x^2 m + \partial_x m V'(m) + \partial_x m\bar{h}\right) \\
&= \left(-\frac{K}{2}(\partial_x m)^2 + V(m) + \bar{h}m\right)\Bigg|_{-\infty}^{+\infty} \\
&= 2\bar{h}\sigma,
\end{aligned} \tag{98}$$

where

$$\sigma \equiv \mathrm{sgn}(m(\infty) - m(-\infty)) \tag{99}$$

determines the parity of the domain wall. This equation obviously cannot be satisfied if one (but not both) of $\widetilde{K}, \bar{h}$ vanish, or when $\mathrm{sgn}(\widetilde{K}) = -\mathrm{sgn}(\bar{h})$ (since the sign of the integral is σ). Even in the case where the signs match however, the integral on the LHS will depend on K and V, which drop out on the RHS; thus for a generic value of parameters no static solution will be possible in this case either.

Since no static solution exists, we expect that a domain wall of this form will propagate ballistically. Assume then that m takes the form $m(x,t) = m(x - R(t))$,

where $R(t)$ is the location of the domain wall. We can then argue that $R(t)$ evolves ballistically by using a similar trick: multiplying (97) by $\partial_x m$ and integrating over space, we have

$$0 = \int_{\mathbb{R}} \left(-(\partial_x m)^2 \partial_t R - \frac{K}{2} \partial_x ((\partial_x m)^2) - \widetilde{K} (\partial_x m)^3 + \partial_x V + \bar{h} \partial_x m \right). \tag{100}$$

This trick is performed because $\partial_x m$ acts effectively as a (signed) delta function that singles out the location of the domain wall $R(t)$. Since the second and fourth terms vanish, we have

$$2\bar{h}\sigma = \int_{\mathbb{R}} \left(\partial_t R + \widetilde{K} \partial_x m \right) (\partial_x m)^2. \tag{101}$$

Ignorning the detailed shape of the domain wall, we may thus take $\partial_x m \to \sigma T(x - R(t))$, where $T(x)$ is an appropriate tophat function. We then conclude that

$$\partial_t R = \sigma(-C\widetilde{K} + D\bar{h}), \tag{102}$$

where C, D are (positive) constants dependent on K and V. Thus domain walls propagate ballistically in a direction determined by $\sigma, \widetilde{K}$, and $\bar{h}$. In particular, a minority domain will either ballistically expand or contract, depending on wether or not the sign of the magnetization in the domain agrees with the sign of $-C\widetilde{K} + D\bar{h}$.

3.1.2 two dimensions

Now consider two dimensions (the extension to $d > 2$ is straightforward). Consider a minority domain with a domain wall at position $R(\theta, t)$, where θ is an angular coordinate in the plane, and assume we may write $m = m(r - R(\theta, t))$. We then switch to polar coordinates, where $\partial_x = \cos\theta \partial_r - r^{-1} \sin\theta \partial_\theta$ and $\partial_y = \sin\theta \partial_r + r^{-1} \cos\theta \partial_\theta$, and $\partial_t m = -\partial_t R \partial_r m$, $\partial_\theta m = -\partial_\theta R \partial_r m$. Then

$$\begin{aligned} -\partial_t R m' = {} & K \left(m'' + \frac{1}{r} m' - \frac{\partial_\theta^2 R}{r^2} m' + \frac{(\partial_\theta R)^2}{r^2} m'' \right) - V'(m) - \bar{h} \\ & + (m')^2 \left((\widetilde{K}_x \cos^2\theta - \widetilde{K}_y \sin^2\theta) + \frac{(\partial_\theta R)^2}{r^2} (\widetilde{K}_x \sin^2\theta - \widetilde{K}_y \cos^2\theta) + 2\cos\theta \sin\theta (\widetilde{K}_x + \widetilde{K}_y) \frac{\partial_\theta R}{r} \right) \end{aligned} \tag{103}$$

where we have saved space by writing m' instead of $\partial_r m$. We then perform the same trick by multiplying both sides of the above equation by m' and integrating over r, taking m' to be a step-like function of sign σ. This gives[8]

$$\begin{aligned} \partial_t R = {} & -BK \left(\frac{1}{R} - \frac{\partial_\theta^2 R}{R^2} + \sigma \frac{(\partial_\theta R)^2}{R^3} \right) + D\sigma\bar{h} \\ & - C\sigma \left((\widetilde{K}_x \cos^2\theta - \widetilde{K}_y \sin^2\theta) + \frac{(\partial_\theta R)^2}{R^2} (\widetilde{K}_x \sin^2\theta - \widetilde{K}_y \cos^2\theta) + 2\cos\theta \sin\theta (\widetilde{K}_x + \widetilde{K}_y) \frac{\partial_\theta R}{R} \right) \end{aligned} \tag{104}$$

where B, D, C are postitive constants dependent on the short-distance profile of the domain wall. When $\widetilde{K}_a = \bar{h} = 0$, this reproduces the slow inward shrinkage of the

[8] Really more terms in this expression can have their own constants, but for us this is not important.

domain wall due to surface tension (the $-BK/R$ term). When $\bar{h}$ or the $\widetilde{K}_a$ are nonzero they give R a constant velocity at large R. Keeping then only the terms that do not vanish at large R, we have

$$\partial_t R = -\sigma \left(C(\widetilde{K}_x \cos^2\theta - \widetilde{K}_y \sin^2\theta) - D\bar{h} \right). \tag{105}$$

In the simplest case where $\widetilde{K}_x = -\widetilde{K}_y \equiv -\widetilde{K}$ and $\bar{h} = 0$, this becomes

$$\partial_t R = -C\widetilde{K}\sigma \cos(2\theta), \tag{106}$$

which correctly reproduces the desired squeezing motion.

3.2 Field theory from the Magnus expansion

We now derive (96) within the context of the time-dependent Glauber dynamics introduced in Sec. 1.4. We will do this using the Floquet driving protocol introduced when discussing the Glauber dynamics implementation. We will assume that ω^{-1} is much longer than the local relaxation time, so that the system's evolution is locally in equilibrium. In this limit we expect the dynamics to be well described by a Langevin equation of the form (ignoring the noise)

$$\partial_t m = (\overline{K}_a + \widetilde{K}_a \cos(\omega t))\partial_a^2 m - (\bar{h} + \widetilde{h}\cos(\omega t)) - V'(m). \tag{107}$$

In the limit where the amplitudes $\widetilde{K}_a, \widetilde{h}$ of the drive are small compared to ω, the micromotion induced by the drive can be effectively rotated away using the Floquet-Magnus expansion, producing an effective Langevin equation driven by a time-independent drift operator. For this to be well-controlled, we need to thus work in the regime

$$\widetilde{J}, \widetilde{h} \ll \omega \ll \overline{J}, \tag{108}$$

with the second inequality coming from the local relaxation time being $\sim 1/\overline{J}$. From our general picture of how squeezing works, we do *not* expect working in this regime to compromise the existence of a threshold.

The Magnus expansion is performed using the techniques of [3], which perform a usual Magnus expansion familiar in quantum mechnaics to the differential operator that appears in the Fokker-Planck equation. We will write the Langevin equation as $\partial_t m = f(m, \omega t)$, with the drift term expanded in Fourier harmonics as

$$f(m, \omega t) = \sum_l f_l(m) e^{il\omega t}. \tag{109}$$

For us only f_0 and $f_1 = f_{-1}$ are nonzero, with

$$f_0 = \overline{K}_a \partial_a^2 m - \bar{h} - V'(m), \qquad f_{\pm 1} = \frac{1}{2}(\widetilde{K}_a \partial_a^2 m - \widetilde{h}). \tag{110}$$

In this case, the results of [3] simplify to give an effective drift force $f_{\text{eff}}(m)$ (with no explicit time dependence) of

$$f_{\text{eff}} = -\frac{1}{\omega^2}[f_1, [f_0, f_1]] \tag{111}$$

to leading order in $1/\omega$, where the commutator is defined as a Lie bracket on field space: for two functionals g, h of m,

$$([g,h])[m(x)] = \int d^d y \left(g[m(y)] \frac{\delta}{\delta m(y)} h[m(x)] - h[m(y)] \frac{\delta}{\delta m(y)} g[m(x)] \right). \tag{112}$$

Note that this expansion is essentially done in $f_{l\neq 0}/\omega$: thus we only require that ω be large compared to the amplitude of the drive, and not necessarily compared to the size of the static part f_0.

To calculate f_{eff}, we use

$$\begin{aligned} [c, V'] &= cV'' \\ [c, \partial_a^2 m] &= 0 \\ [\partial_a^2 m, \partial_b^2 m] &= 0 \\ [\partial_a^2 m, V'] &= -(\partial_b m)^2 V''', \end{aligned} \tag{113}$$

where c stands for the constant operator (for us either $\widetilde{h}$ or $\bar{h}$).[9] Then one derives

$$[f_0, f_1] = -\widetilde{h} V'' - \widetilde{K}_b (\partial_b m)^2 V'''. \tag{114}$$

Taking the commutator of this with f_1,

$$[f_1, [f_0, f_1]] = 2\widetilde{h}\widetilde{K}_a (\partial_a m)^2 V'''' + \widetilde{h}^2 V''' - \widetilde{K}_a \widetilde{K}_b [\partial_a^2 m, (\partial_b m)^2 V'''']. \tag{115}$$

Evaluating the last commutator under the simplifying assumption that $\delta^5 V/\delta m^5 = 0$ and collecting terms, we arrive at[10]

$$\begin{aligned} \partial_t m = \overline{K}_a \partial_a^2 m - \bar{h} - \left(V' + \frac{\widetilde{h}^2}{\omega^2} V''' \right) - \lambda_a (\partial_a m)^2 \\ - 2\widetilde{K}_a \widetilde{K}_b \left(2\partial_a^2 \partial_b m \partial_b m V''' + 2\partial_a m \partial_b m \partial_a \partial_b m V'''' + (\partial_a \partial_b m)^2 V''' \right) \end{aligned} \tag{116}$$

where

$$\lambda_a \equiv \frac{2\widetilde{h}\widetilde{K}_a V''''}{\omega^2}. \tag{117}$$

This yields (96) together with additional interactions that are unimportant for determining the qualitative behavior of the coarsening dynamics.

[9] The second line comes from $([c, \partial_a^2 m])[m(x)] = c \int_y \partial_{a,y}^2 \delta(x-y) = 0$.

[10] If we were to keep track of the noise as well, we would find a renormalization of the diffusion constant. Since we are in any case not assuming FDT, this renormalization will not be important to explicitly calculate.

4 Phase diagrams

In this section we numerically calculate phase diagrams of the models $\mathsf{S}_{2,3}$, in various dimensions and with different types of updates, and compare the results with the predictions of the extended mean field theories developed above.

4.1 Generalities

We will identify phase transitions by plotting a normalized version of the Binder cumulant

$$B = \frac{3}{2}\left(1 - \frac{\langle M^4\rangle}{3\langle M^2\rangle^2}\right), \tag{118}$$

where the total magnetization is $M = \sum_i m_i$ and the expectation value is taken in the non-equilibrium steady state. B is a function of the kurtosis of the magnetization $K_M \equiv \langle M^4\rangle/\langle M^2\rangle^2$. $K_M \geq 1$,[11] so $B \leq 1$. We also know that $K_M = 3$ for a Gaussian distribution (since the number of distinct ways to contract the four Ms is $\frac{1}{2}\binom{4}{2} = 3$). Therefore we in general expect B to be close to 1 at small error rates—where the fluctuations are small, so that $\langle M^4\rangle \approx \langle M^2\rangle^2$—and to be close to zero at large error rates, where the correlation length is small and the distributions of extensive variables (such as M) become narrow Gaussians. Negative values of B mean that the magnetization has a distribution with tails fatter than that of a Gaussian, which can occur at intermediate noise rates near the transition.

We will also find it useful to analyze the susceptibility

$$\chi = \frac{1}{L^d}(\langle M^2\rangle - \langle |M|\rangle^2), \tag{119}$$

which will be used to attempt to extract the critical exponents. The factor of $1/L^d$ in front ensures that $\chi = O(1)$ away from the critical point (although emperically the location of the divergence in χ is a less reliable indicator of the phase transition than the crossing point of B).

We will attempt to identify the critical exponents ν, χ, β through the scaling forms

$$B(t, L) = \phi_B(tL^{1/\nu}), \qquad \chi(t, L) = L^{\gamma/\nu}\phi_\chi(tL^{1/\nu}), \qquad |m| = L^{-\beta/\nu}\phi_m(tL^{1/\nu}), \tag{120}$$

where $t \equiv (p - p_c)/p_c$ and $\phi_B, \phi_\chi, \phi_m$ are scaling functions. The usual hyperscaling relations means that knowledge of two of these exponents (or any other pair) is sufficient to obtain all other exponents.

All plots shown below will be at unbiased noise (for biased noise we expect a first order transition in all cases). A summary of the results is shown below, where a $\times$ indicates that no transition occurs (the model is disordered at any nonzero p)

p_c	$\mathsf{S}_2^{\text{asynch}}$	$\mathsf{S}_3^{\text{asynch}}$	$\mathsf{S}_2^{\text{synch}}$	$\mathsf{S}_3^{\text{synch}}$
$2d$	.039	.030	?	.15
$3d$	$\times$	$\times$	.016	?
$4d$	.024	$\times$	?	?

[11] This is just Jensen's inequality.

4.2 S_2 rule

We start with S_2, which from our previous analysis, we expect will generally have a higher threshold than S_3.

4.2.1 2d—asynchronous updates

The first thing to check is that S_2, operating under asynchronous updates, has a high probability of working as a reliable eroder. We can do this by running S_2 on random initial states with magnetization $1-2p_{\text{init}}$, where p_{init} is thought of as the probability of having an error in the initial state, and computing the expected value of the late-time magnetization $\langle m_\infty \rangle$. Doing this gives

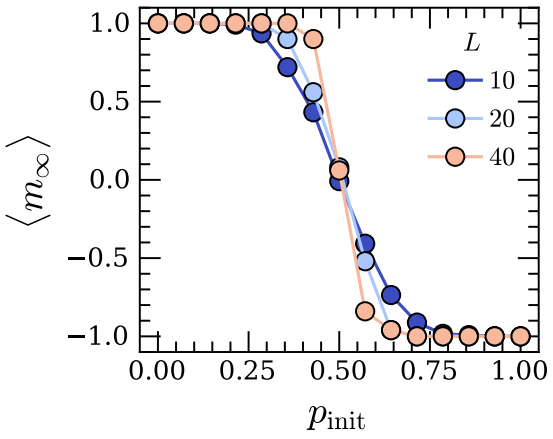

(121)

which shows that S_2 indeed operates as an eroder even when it lacks synchronicity.

We then compute B and χ, finding a transition around $p_c^{2d} \approx 0.039$:

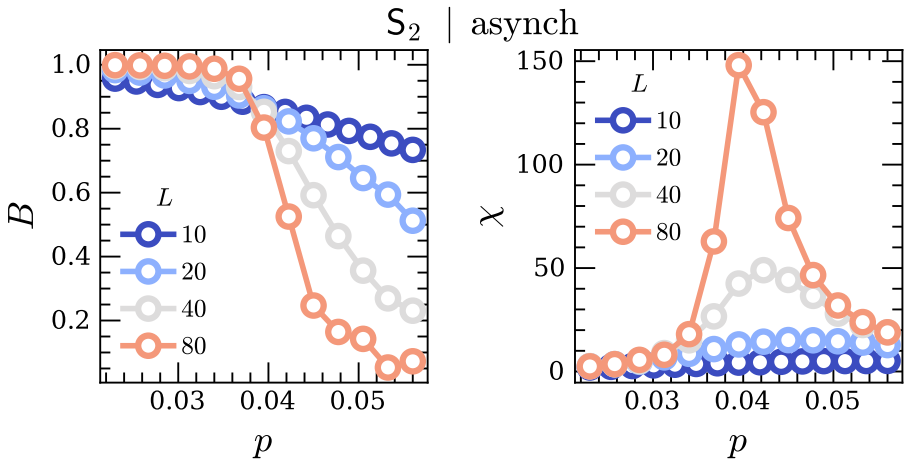

(122)

$p \approx 0.039$ is also the location at which the threshold in the relaxation time τ onsets.

Trying our best to collapse this gives ethan: *all of the figures of χ should actually have y*

labels of $L^{-\gamma/\nu}\chi$

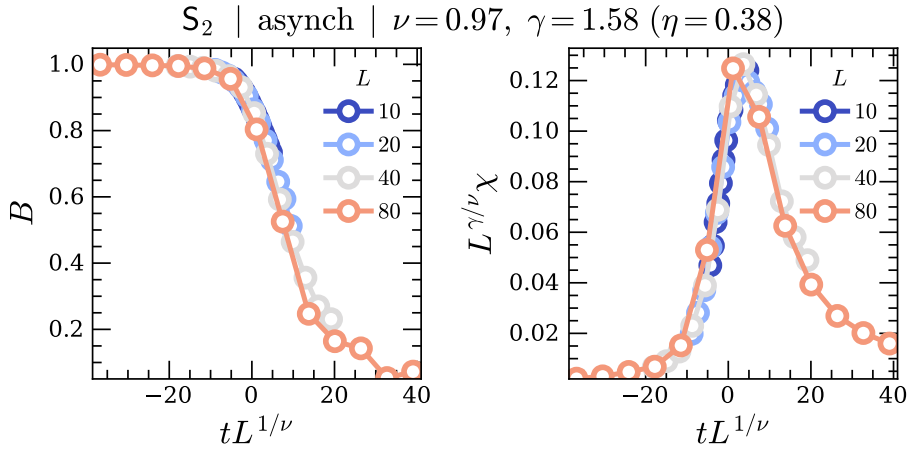

(123)

which is actually fairly close to the Ising value of $\gamma_I = 7/4$.

4.2.2 3d—asynchronous updates

In three dimensions with asynchronous updates we expect either a first order transition, or the absence of an ordered phase entirely. The transition, if it exists, will be invisible in the infinite-time steady state dynamics, which even at zero bias will have a nonzero magnetization fixed by the asymmetry of the squeezing rule (this is in contrast to the second-order case, where the transition can be identified by computing the susceptibility / Binder cumulant in the long-time steady state). We thus look instead at the scaling of τ for initial states with magnetization aligned against the bias of the squeezing rule.

Doing this indicates that there is *no* threshold for asynchronous updates, with $\tau \sim 1/p$ independently of L (note the log scale) (note: x axis should be p)

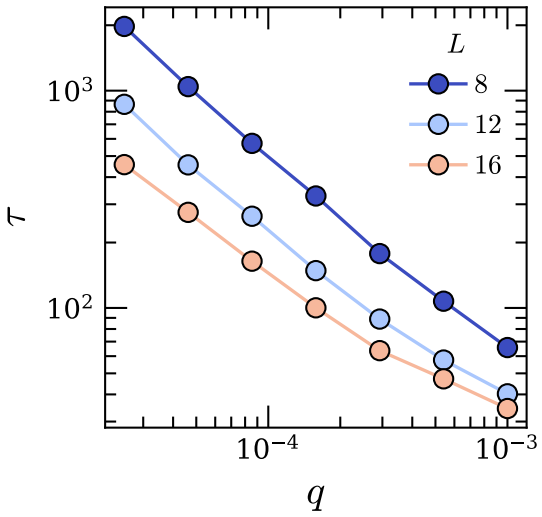

(124)

This claim is substantiated by showing that S_2 fails to function as an eroder in 3d. With our choice of updates (two $\wedge$s and one $\vee$), the system is biased towards negative

magnetizations. Therefore in the TDL, we expect $\langle m_\infty \rangle \to -1$ for all p_{init} if S_2 fails to function as an eroder. Indeed, we find

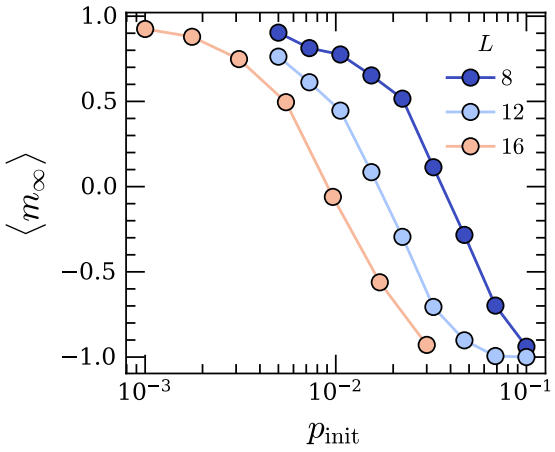

(125)

Thus in 3d, synchronicity breaking destroys the transition.

4.2.3 4d—asynchronous updates

For unbiased noise we expect a continuous transition. Indeed, in the present case we find a transition around $p_c^{4d} \approx 0.024$, which while significantly lower than p_c^{2d} (in accordance with $p_c \sim 1/d^2$) is still clearly nonzero:

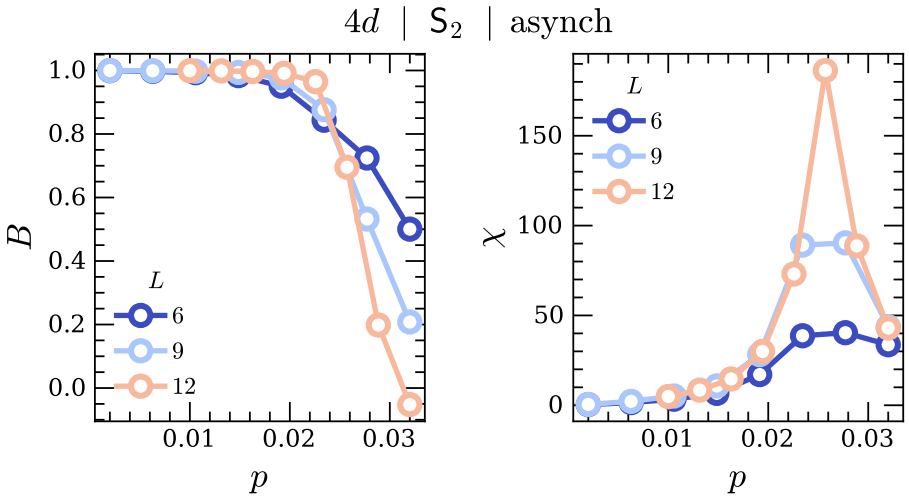

(126)

One may also check that S_2 *does* function as a good eroder in 4d. A collapse to the mean field values of $\nu = 1/2, \gamma = 1$ is okay, but not great (smaller ν work better).

4.2.4 2d—synchronous updates

Synchronous updates for this model are observed to be much noiser than asynchronous ones for this model, and for the current low-budget effort we will not try to pin down

p_c using B/χ, but rather by looking at τ. This gives a transition near $p_c^{2d,synch} \sim 0.09$

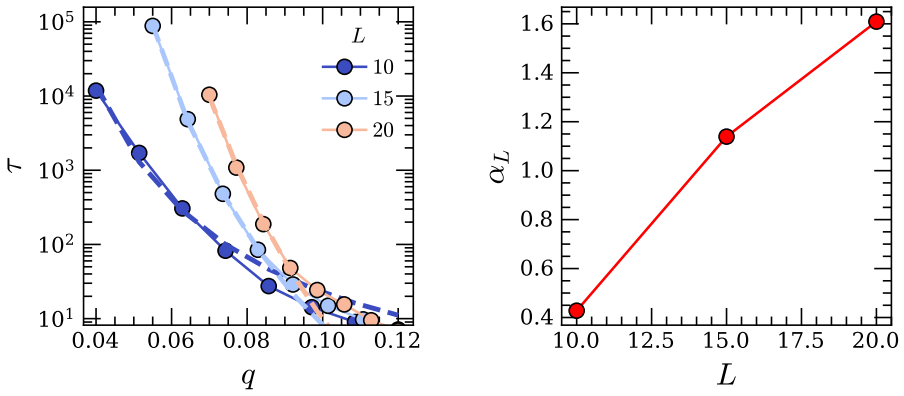

(127)

although we clearly need to get more serious data to estimate p_c better (in particular this value would give a smaller value for p_c for S_2 than S_3 in the synchronous case, but not in the asynchronous case).

4.2.5 3d—synchronous updates

Since S_2 is an eroder under synchronous updates, we know there must exist a threshold. Indeed, our low-budget numerics identify one around $p_c^{3d,synch} \approx 0.016$:

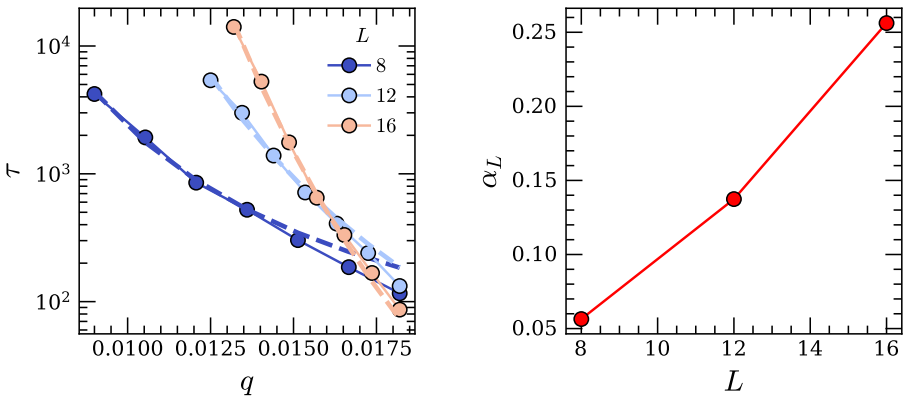

(128)

While it is not necessary, one may also check that S_2 *does* erode initial errors when the updates are synchronous. Since the breaking of the $\mathbb{Z}_2$ symmetry favors states with negative magnetization, we expect plots of $\langle m_\infty \rangle$ for different L to cross at a value of

initial errors $p_{\text{init}} < 0.5$. Indeed, we find a crossing around $p_{\text{init}} \approx 0.15$:

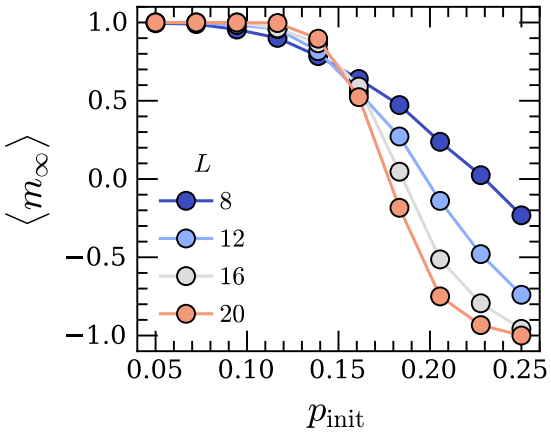

(129)

4.2.6 4d—synchronous updates

In 4d, asychronous updates were observed to yield a transition whose exponents may be consistent with mean field values, as one would naively expect. What about for synchronous ones?

The result appears slightly strange: B shows a very sharp dip around the location of a divergence in χ, and an attempt at a scaling collapse (with a guess of $p_c = 0.155$) yields

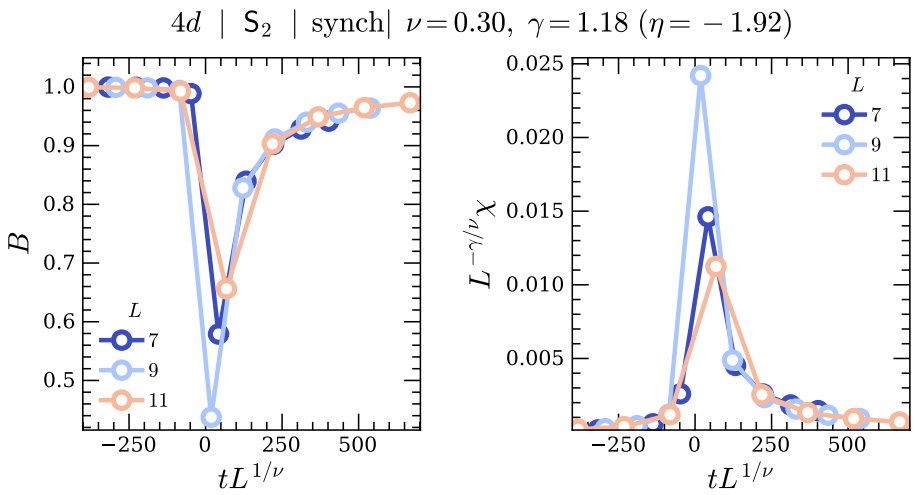

(130)

This is quasi-close to the mean-field values of $\nu = 1/2, \gamma = 1$, but more rigorous numerics will be required to know for sure.

4.3 S_3 rule

Now we consider S_3. Our previous analysis indicated that S_3 should have a lower threshold than S_2, and this is indeed what we observe in the numerics. Like S_2, S_3 fails to have a threshold in 3d for asynchronous updates. More importantly however, S_3 also has no threshold for asynchronous updates in 4d. This shows that the S_3 model with asynchronous updates orders *only* in two dimensions.

4.3.1 2d—asynchronous updates

For unbiased noise we find a transition around $p_c^{2d} \approx 0.0296$:

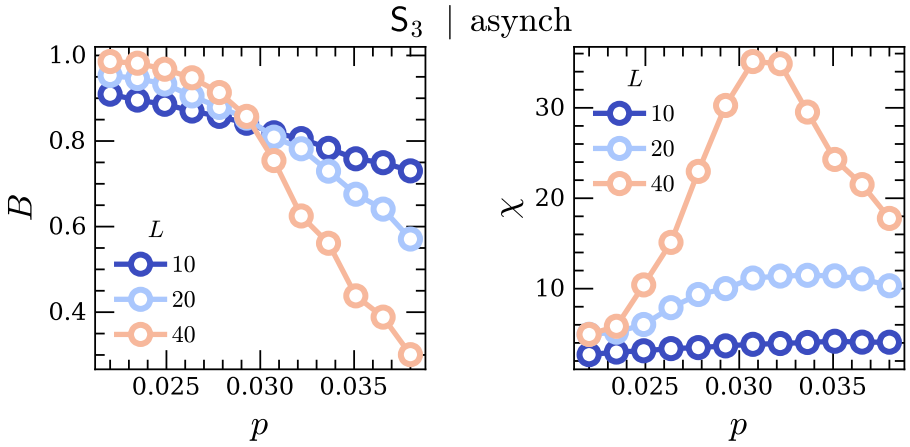

(131)

This is a fair bit lower than the critical point for S_2 in the same situation, which is consistent with our mean field and operator-based analysis above. Collapsing this gives

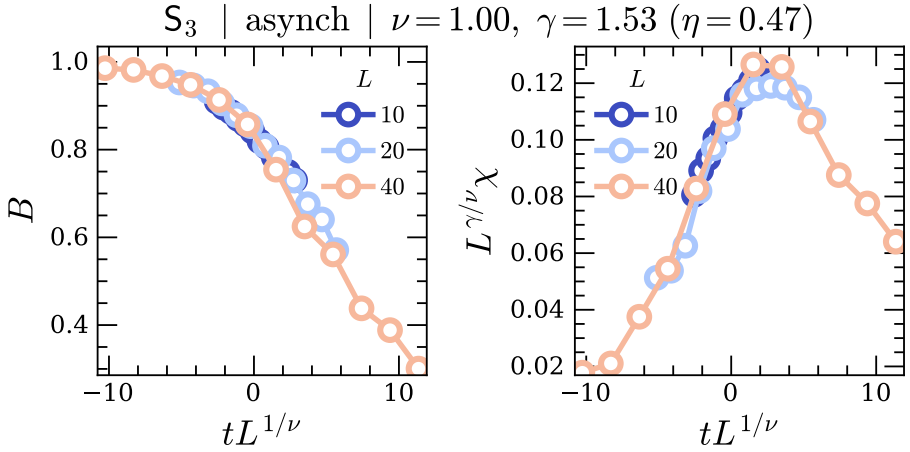

(132)

which gives η reasonably close to 1/2; fits to Ising exponents do not work very well.

4.3.2 3d—asynchronous updates

Given that S_2 is disordered under asynchronous updates in 3d, we expect the same to be true for S_3. For this it is sufficient to compute $\langle m_\infty \rangle$ and show the absence of a

threshold as a function of p_{init}. Doing this gives a plot very similar to the S_2 case:

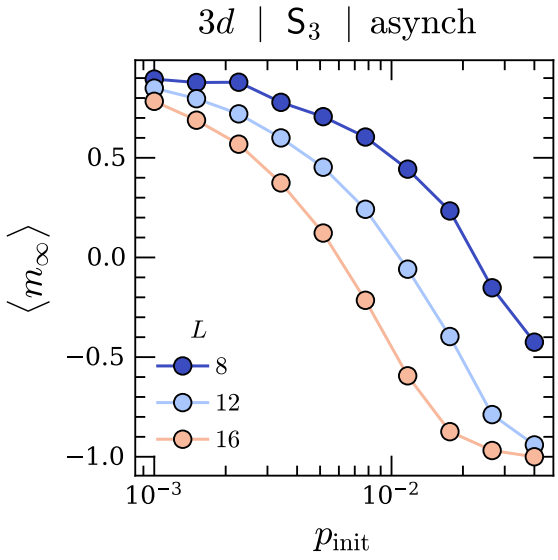

(133)

4.3.3 4d—asynchronous updates

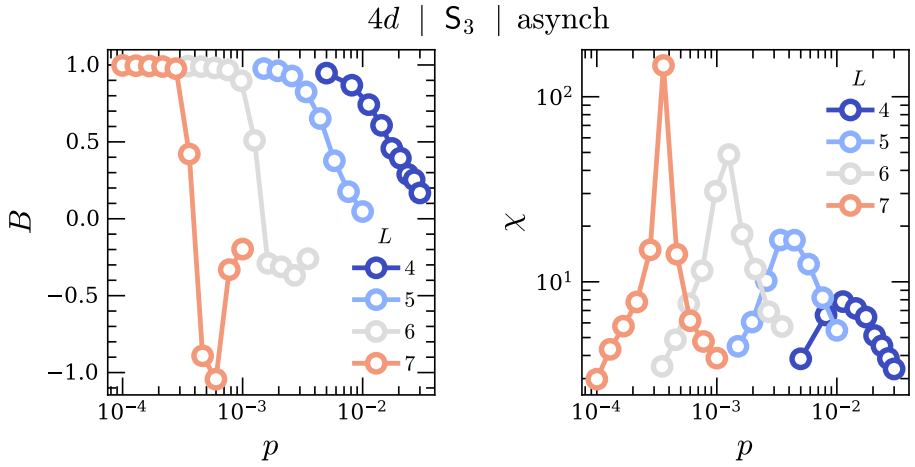

(134)

Given that $p_c \to 0$ in the TDL, it is natural to wonder how well S_3 erodes errors in initial states. The generalization of Toom's theorem to the asynchronous case would say that if an asychronous CA A is such that $\mathsf{A}, \mathsf{A}^\vee$ are both eroders in the TDL with probability 1 (over realizations of update patterns), then A has a phase transition at an $O(1)$ error rate (the converse, viz. that a model with a robust phase transition must be an asynchronous eroder, is of course true).

Now if this generalization of Toom's result is true, we expect S_3 to *not* be an eroder

in the TDL. This is indeed in accordance with numerics, which finds

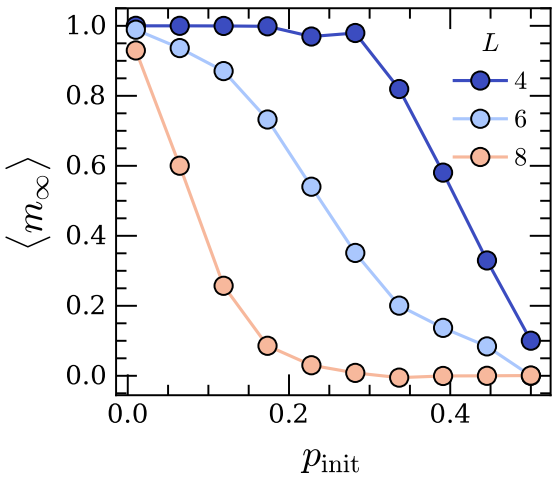

(135)

4.3.4 2d—synchronous updates

Making the updates synchronous increases the threshold by a factor of about 5 to $p_c^{2d,synch} \approx 0.15$:

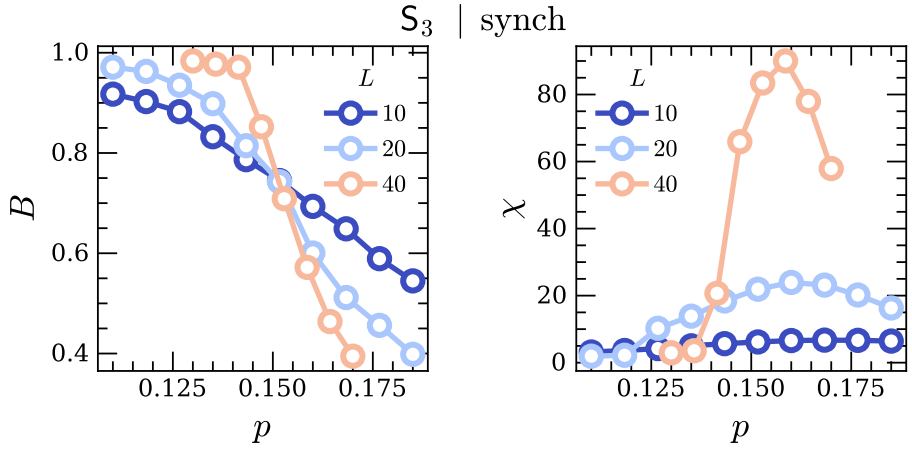

(136)

The current low-budget numerics give the following (rather poor) scaling "collapse":

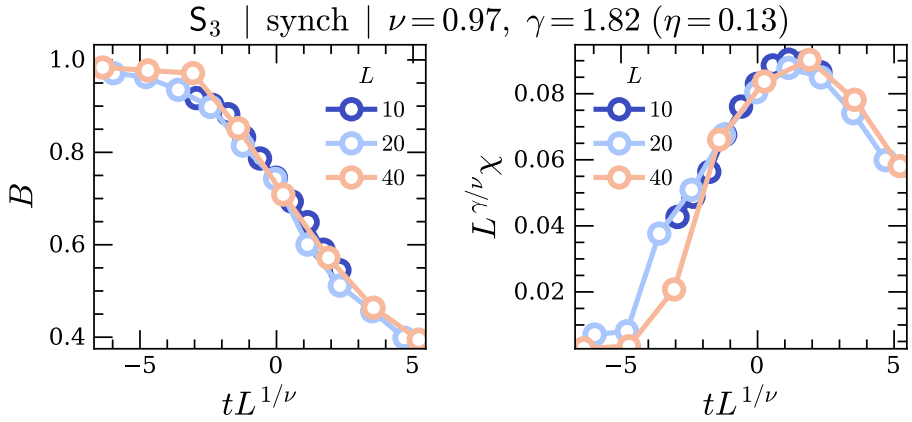

(137)

One may also ask what happens when one applies synchronous updates, but breaks time translation symmetry. We will address this by looking at what happens when at each time step, synchronous $\vee$ or $\wedge$ updates are applied randomly (with equally-chosen probabilities).

Doing this is observed to reduce p_c by around a factor of 10, to a value near that of the completely asychronous updates, although the crossing of B and the peaks in χ seem to be fairly well-separated at small L:

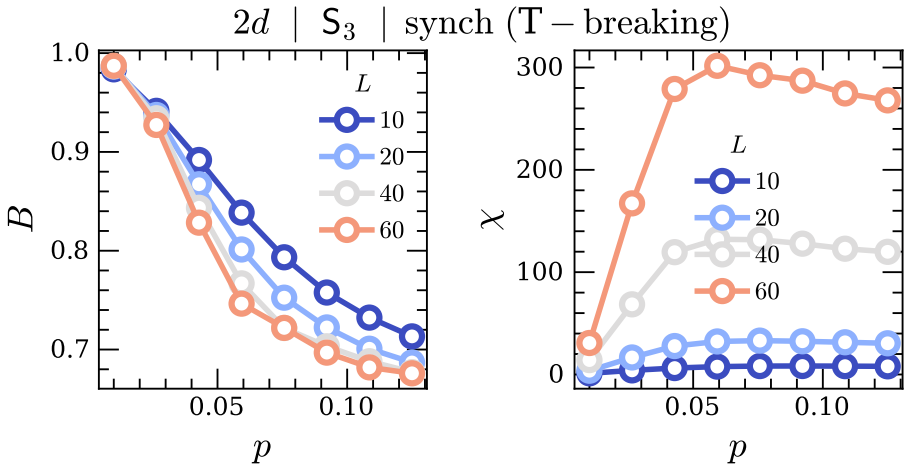

(138)

Collapsing this can be done, but yields very large values of ν, γ:

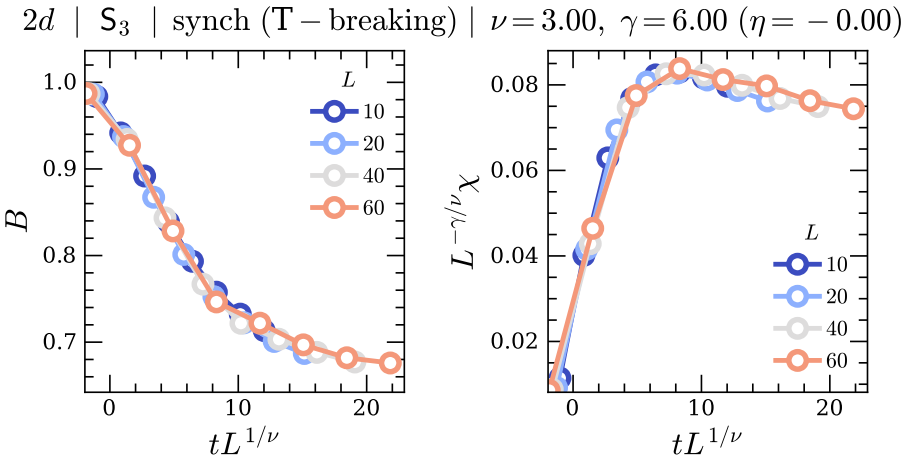

(139)

It thus appears that getting rid of exact time translation invariance changes the universality class of the transition.

4.3.5 4d—synchronous updates

Low-budget numerics for the synchronous case gives a rather unusual Binder ratio behavior:

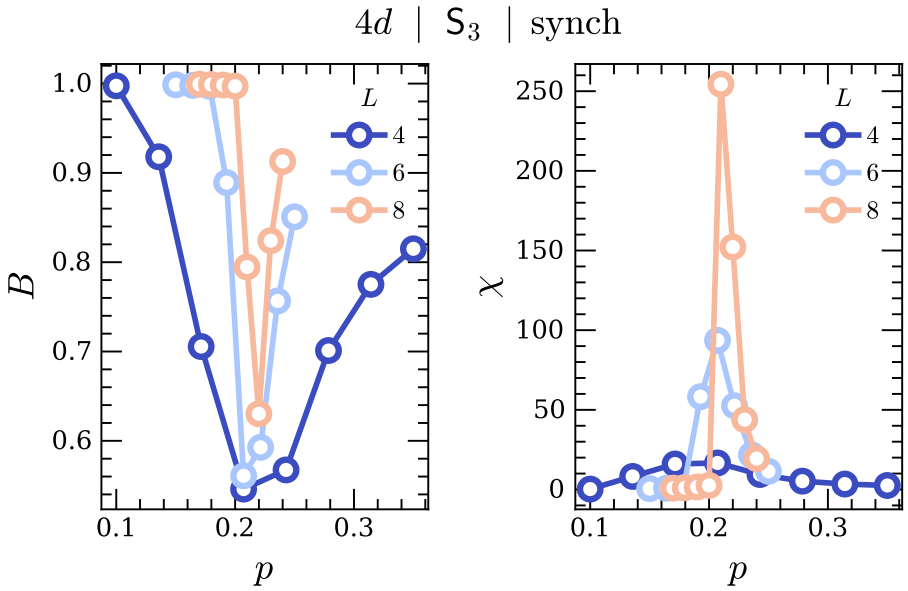

(140)

A crude scaling collapse on this data actually works surprisingly well (with $p_c \approx 0.2$ as identified by the B crossing [although it occurs near the minimum in B]), but the standard hyperscaling relations would give $\eta \approx -2$. Could it be that the transition in 4d is not mean field like?

5 Miscellaneous things

5.1 Adding noise

The Langevin equations derived above did not contain a noise term, although the addition of one is straightforward. We use the generating functional approach by defining

$$W[\Gamma] = \langle e^{\sum_{i,t} \Gamma_{i,t} \Delta_{i,t}} \rangle, \tag{141}$$

where as usual $\langle \cdot \rangle$ is in the non-eq steady state, and $\Delta_{i,t}$ is the "jump field" $s_{i,t+1} - s_{i,t}$. For simplicity we will just work with the rule S_2. In terms of the probabilities used to write down the master equation above, one finds

$$\begin{aligned} W[\Gamma] = \exp \Bigg(& \frac{1}{N} \sum_{i,t} (e^{\Gamma_{i,t}} - 1)(1 - P_{i,t}) \left(\frac{1-p}{2} (P_{i,t}^{N \wedge S} + P_{i,t}^{E \vee W}) + \frac{p}{2}(1+\eta) \right) \\ & + \frac{1}{N} \sum_{i,t} (e^{-\Gamma_{i,t}} - 1) P_{i,t} \left(2 \frac{1-p}{2} (2 - P_{i,t}^{N \wedge S} - P_{i,t}^{E \vee W}) + \frac{p}{2}(1-\eta) \right) \Bigg) \end{aligned} \tag{142}$$

Since $\ln W$ generates connected correlation functions of $\Delta_{i,t}$, we can find the required noise correlators by differentiating twice with respect to $\Gamma_{i,t}$. After doing this and writing things in terms of m, we have

$$\begin{aligned} \langle \partial_t m_{i,t} \partial_{t'} m_{j,t'} \rangle_c = 2 \delta_{t,t'} \delta_{i,j} \Big(& 1 - p\eta m_i \\ & + \frac{1-p}{4} (m_{i+y} + m_{i-y} + m_{i+x} + m_{i-x} + m_{i+y} m_{i-y} - m_{i+x} m_{i-x}) m_i \Big). \end{aligned} \tag{143}$$

Therefore if $\xi_{i,t}$ is the noise added to the above deterministic Langevin equation for m, $\langle \xi_{i,t} \xi_{j,t'} \rangle$ must be equal to the RHS.

5.2 Heating

Maintaining memory in our models requires the breaking of detailed balance, viz. a net flow of heat dissipation to the environment (a bath at temperature $1/\beta$) to be maintained. We can quantify the amount of heat flow dQ by using the fact that after an update $P(A \to B)$ between two configurations A, B, the entropy dissipated into the environment is

$$dS(A \to B) = \ln \frac{P(A \to B)}{P(B \to A)}, \tag{144}$$

with $dS = \beta dQ$. The sign conventions here are such that when the system relaxaes towards more likely states it dissipates heat to the environment ($dQ > 0$); moving to less likely states by contrast requires injection of heat from the environment ($dQ < 0$).

Note that heat transfer is a kind of holonomy, since dQ is essentially a derivative on configuration space: heat transfer comes only from the "area enclosed" by paths in configuration space. For example, any process $A \to B \to A$ is easily checked to result in zero net heat exchange, since $dQ(A \to B) = -dQ(B \to A)$.

Consider a system with a time-periodic markov generator $\mathcal{M}_t$, whose updates obey detailed balance with respect to a time-dependent energy function E_t, so that

$$\ln \frac{P(A \xrightarrow{t} B)}{P(B \xrightarrow{t} A)} = \beta(\langle E_t|A\rangle - \langle E_t|B\rangle). \tag{145}$$

We will let $|\pi_t\rangle$ denote the (non-equilibrium) steady state at time t, with expectation values of quantities being obtained by taking inner products with $|\pi_t\rangle$ (e.g. the average energy at time t in the steady state is $\langle E_t|\pi_t\rangle$). Then the expected value of the heat transfer in the non-equilibrium steady state at time t is

$$\begin{aligned}\langle dQ_t\rangle &= \sum_{A,B}\langle\pi_t|A\rangle\langle A|\mathcal{M}_t|B\rangle(\langle E_t|A\rangle - \langle E_t|B\rangle) \\ &= \langle\pi_t|\mathbf{1} - \mathcal{M}_t|E_t\rangle.\end{aligned} \tag{146}$$

where $\langle dQ_t\rangle$ indicates expectation value in the non-equilibrium steady state. Now if the Markov process was time-independent we would have $\langle\pi_t|\mathcal{M} = \langle\pi_t|$, and hence would correctly recover $\langle dQ_t\rangle = 0$. As it is, for a time step dt we instead have $\langle\pi_t|\mathcal{M}_t = \langle\pi_{t+dt}|$[12], and so

$$\langle\partial_t Q\rangle = -\langle\partial_t\pi|E_t\rangle. \tag{147}$$

Letting the period of the Markov generator be τ, the average heat dissipation rate over a period is

$$\beta\langle\Delta Q\rangle = \frac{1}{\tau}\int_0^\tau dt\,\langle\pi_t|\partial_t E_t\rangle, \tag{148}$$

viz. $\langle\Delta Q\rangle$ is just the time-averaged expectation value of $\partial_t E_t$.

In the stochastic error model, where $\mathcal{M}_t$ is independent of t but does not obey detailed balance, we just calculate dQ directly using the update probabilities. For example, the probability of making a spin flip for the two-control-spin squeezing rule S_2 is

$$\begin{aligned}P(s_i \to -s_i) = p\frac{1-s_i\eta}{2} + \frac{1-p}{2}\Bigg[&\frac{1+s_i}{2}\left(\frac{(1-s_{i+x})(1-s_{i-x})}{4} + \frac{3-s_{i+y}-s_{i-y}-s_{i+y}s_{i-y}}{4}\right) \\ &+ \frac{1-s_i}{2}\left(\frac{(1+s_{i+y})(1+s_{i-y})}{4} + \frac{3+s_{i+x}+s_{i-x}-s_{i+x}s_{i-x}}{4}\right)\Bigg]\end{aligned} \tag{149}$$

[12]This fact probably does not deserve proof, but just in case. Let $\mathcal{M}_a^b \equiv \mathcal{M}_b\cdots\mathcal{M}_a$, where we set $dt = 1$ and let $a, b \in \{1,\ldots,\tau\}$. In the steady state, we have $(\mathcal{M}_a^{\tau+a})^n = |\pi_a\rangle\langle\pi_a|$ for $n \to \infty$. Multiplying both sides of this equation on the left by $\mathcal{M}_a$ and on the right by $\mathcal{M}_a^T$ gives $(\mathcal{M}_{a+1}^{\tau+a+1})^n = |\mathcal{M}_a\pi_a\rangle\langle\mathcal{M}_a\pi_a|$, and so $\mathcal{M}_a|\pi_a\rangle = |\pi_{a+1}\rangle$.

References

[1] C. H. Bennett and G. Grinstein. Role of irreversibility in stabilizing complex and nonergodic behavior in locally interacting discrete systems. Physical review letters, 55(7):657, 1985.

[2] G. Grinstein, C. Jayaprakash, and Y. He. Statistical mechanics of probabilistic cellular automata. Physical review letters, 55(23):2527, 1985.

[3] S. Higashikawa, H. Fujita, and M. Sato. Floquet engineering of classical systems. arXiv preprint arXiv:1810.01103, 2018.

[4] A. Kubica and J. Preskill. Cellular-automaton decoders with provable thresholds for topological codes. Physical review letters, 123(2):020501, 2019.

[5] L. Ponselet. Phase transitions in probabilistic cellular automata. arXiv preprint arXiv:1312.3612, 2013.

[6] A. Ray, R. Laflamme, and A. Kubica. Protecting information via probabilistic cellular automata. Physical Review E, 109(4):044141, 2024.

[7] K. Takeuchi. Can the ising critical behaviour survive in non-equilibrium synchronous cellular automata? Physica D: Nonlinear Phenomena, 223(2):146–150, 2006.

[8] A. L. Toom. Stable and attractive trajectories in multicomponent systems. Multicomponent random systems, 6:549–575, 1980.